Latitudinal Variation in the Growth and Condition of Juvenile Flatfishes in the Bering Sea

Cynthia Yeung*[1], Louise A. Copeman[1], Mary E. Matta[1], Mei-Sun Yang[1]

*Corresponding author: cynthia.yeung@noaa.gov

[1]National Oceanic and Atmospheric Administration
National Marine Fisheries Service
Alaska Fisheries Science Center
7600 Sand Point Way NE
Seattle, Washington 98115
U.S.A.

ABSTRACT

The Bering Sea spans a wide latitudinal range, connecting with the temperate North Pacific Ocean to the south and the arctic Chukchi Sea to the north. Climate change has rapidly and significantly altered Bering Sea ecosystem dynamics. The biomass of predominantly boreal marine species have increased in the subarctic northern Bering Sea following recent record-high water temperatures across the shelf. Among those species are two commercially-important flatfishes: yellowfin sole (*Limanda aspera*; YFS) and northern rock sole (*Lepidopsetta polyxystra*; NRS). In this study, the Bering Sea was divided latitudinally into three areas – north, central, and south – to assess the implications of a northward shift or expansion of juvenile flatfish habitat on production potential. The growth, diet, and condition of juveniles were compared among areas from 2016 to 2018. Summer bottom temperatures in the Bering Sea in 2016 and 2018 were anomalously warm, but 2017 temperatures were closer to the 2010 – 2018 average. Prey availability does not appear to be a limiting habitat factor across the Bering Sea. Juveniles of both species grow faster in length and to greater length-at age in the south. The morphometric-based condition of juvenile YFS appears to be better in the northern Bering Sea, while that of juvenile NRS also improves towards the north. Condition increased from 2016 to 2017, but then decreased slightly from 2017 to 2018. Although the results suggest larger size and faster growth of juveniles are associated with warmer bottom temperatures, there is also indication that growth and condition of juvenile flatfish may not continue to increase if current high temperatures persist in their habitat. Exploratory habitat models show that the condition of juvenile YFS may be negatively influenced by temperature. Negative effects on growth and energy storage may set in as the upper thermal physiological tolerance of each species is approached. The critical temperature maxima for each species is unknown, but it may be lower for the cold-adapted YFS than for NRS, implying that YFS may be less buffered against effects of climate warming.

KEYWORDS

habitat; climate change; ecosystem; juvenile growth; subarctic; temperature; USA, Alaska, Bering Sea

RUNNING HEAD

Juvenile flatfishes growth and condition

1 INTRODUCTION

The broad continental shelf of the Bering Sea in Alaska contributes almost 60% of total landings and a third of the total value of United States fisheries (National Marine Fisheries Service, 2020). Fishing activity is mostly limited to the boreal eastern Bering Sea (54 – 60°N) with low levels of commercial, subsistence and recreational fishing in the subarctic northern Bering Sea (60 – 66°N) (Figure 1) (Renner and Huntington, 2014). Sea ice dynamics are the main drivers that functionally separate the northern and eastern Bering Sea ecosystems (Stabeno et al., 2012). Secondary production in the northern Bering Sea ecosystem is driven by ice-associated phytoplankton production as well as spring pelagic phytoplankton production, with the bloom seeded by melting winter sea ice (Brown and Arrigo, 2013). Melting sea ice also results in the formation of the "cold pool", a layer of cold (<2°C) water that forms below the pycnocline over the middle shelf domain of the eastern Bering Sea (50 to 100 m depth) during sea ice retreat (Wyllie-Echeverria and Wooster, 1998). Previous studies have proposed that the cold-pool serves as a physical barrier to the migration of boreal groundfish and invertebrates from the eastern Bering Sea (Hollowed et al., 2013). However, climate change has resulted in a drastic loss of sea ice, with reduced areal extent and thickness as well as later fall formation and earlier spring retreat (Grebmeier, 2012; Huntington et al., 2020; Stabeno and Bell, 2019). The diminished influence of the cold pool in the eastern Bering Sea and sea ice in the northern Bering Sea have moved the two ecosystems towards becoming connected as one (NPFMC, 2018).

Since a warm thermal stanza across the Bering Sea began in late 2013, there has been a series of recording-breaking high water temperatures (Stabeno et al., 2019) that are affecting Bering Sea ecosystem functions at all trophic levels (Duffy-Anderson et al., 2019; Mueter et al., 2012). Among the most conspicuous changes is the increased biomass of predominantly boreal species in the northern Bering Sea, including the commercially-important groundfishes walleye pollock (*Gadus chalcogrammus*), Pacific cod (*Gadus macrocephalus*), yellowfin sole (*Limanda aspera*) and northern rock sole (*Lepidopsetta polyxystra*) (Stevenson and Lauth, 2019). Some species, such as Pacific cod and walleye pollock, have

increased in abundance in the northern Bering Sea due to movement of adults and juveniles, while others, such as northern rock sole, seem to have increased due to successful recruitment of benthic juveniles which have grown and remained in the northern Bering Sea (Eisner et al., 2020; Stevenson and Lauth, 2019).

Northern rock sole (NRS) and yellowfin sole (YFS) are highly abundant and economically valuable flatfishes in the eastern Bering Sea. The YFS fishery in the eastern Bering Sea is the largest flatfish fishery in the world (Spies et al., 2019). Both flatfishes have diets that mostly consist of benthic prey (Yeung and Yang, 2018). Data on these flatfishes in the Bering Sea primarily consist of empirical observations of spatial distributions (e.g., Cooper and Nichol, 2016; Nichol et al., 2019), while the ecological processes that influence their growth and condition are not well studied, particularly during the juvenile stage (NPFMC, 2017). The distribution of juvenile NRS lies mainly in the eastern Bering Sea, whereas the distribution of juvenile YFS is relatively offset towards the north and extends into the northern Bering Sea (Yeung and Cooper, 2019). A northward expansion of their habitat range could increase the recruitment and biomass production of the stocks if the added habitat is of suitable quality (e.g., food, temperature, predators) (Amara et al., 2007; Gibson, 1994).

Habitats with favorable temperature and high prey abundance are expected to produce fish with higher energy reserves or faster growth, thereby increasing survival (De Raedemaecker et al., 2012; Gibson, 1994). Substrate type, usually defined by grain-size distribution of the surficial sediment, is also a key attribute of suitable flatfish habitat because of its influence on the benthic infauna prey community (Feder et al., 2007) and the burial capability of juvenile flatfishes (Stoner and Titgen, 2003; Yeung and Yang, 2017). In this study, the latitudinal extent of the Bering Sea inner shelf (< 50 m deep) was divided into three areas. The growth, diet, and condition of juvenile flatfish were compared among the areas in relation to temperature, substrate, and prey availability. The objective was to identify latitudinal variation in habitat quality that could affect juvenile biomass production in a scenario of northward range shift or

expansion. Interspecific comparison may facilitate insights into the juvenile dynamics of two flatfish species that occupy similar ecological niches, sharing comparable diets and spatial distributions. This is the first study comparing the growth and condition of juvenile flatfishes in natural field settings across a latitudinal gradient in the Bering Sea.

2 METHODS

2.1 Study area

The Alaska Fisheries Science Center (AFSC) conducts an annual summer (June – August) bottom trawl survey in the eastern Bering Sea shelf to assess groundfish and invertebrate stocks (Lauth et al., 2019). In 2017, the survey was extended into the northern Bering Sea as part of the National Oceanic and Atmospheric Administration (NOAA) Arctic initiative to monitor ecosystem changes induced by climate change (NOAA, 2014). To compare the spatial variability in the characteristics of juvenile flatfish (age, length, diet, growth, and condition) and their habitat (temperature, prey availability, substrate), the inner shelf of the Bering Sea was divided latitudinally into three areas for analysis (Figure 1). In addition to the (1) northern Bering Sea, defined as north of latitude 60.4^{o} according to survey convention, the eastern Bering Sea was divided at latitude 58.4^{o} into the (2) central (Kuskokwim Bay) and the (3) southern (Bristol Bay) areas, which are distinctively important for fisheries management (Halas and Neufeld, 2018; McDevitt et al., 2020). These areas will be referred to as north, central, and south hereinafter.

2.2 Data collection

2.2.1 Fish sampling

Juvenile NRS and YFS were collected during the 2016 – 2018 surveys. Juveniles are defined here as fish of total length (*TL*) ≤20 cm, which is the size of the specimens targeted in this study. Most (99%) of the juveniles collected were actually ≤15 cm. Hereinafter, reference to NRS and YFS from this study implies juveniles, and length is *TL* unless otherwise specified.

Two different fishery-independent sampling methods were used. The standard survey sampling gear is an 83-112 eastern bottom trawl with a 25.3 m long headrope and a 34.1 m long footrope. The mesh size varies from a maximum of 10.2 cm in the wings and throat to a minimum of 3.2 cm for the liner in the codend. The bottom trawl is designed to target adult fish and is not efficient at catching fish of length <14 cm or small macrobenthic fauna (Kotwicki et al., 2017). Small fauna that are retained are often damaged. Therefore, a 3-m plumb-staff beam trawl (Abookire and Rose, 2005) was also deployed specifically to collect intact juvenile flatfish specimens to study their growth and physiological condition in relation to the habitat.

Specimens for this study were collected at a subset of standard bottom trawl survey stations on the inner shelf (depth ≲50 m) (Figure 1) mainly with the beam trawl (10 – 20 min duration), and opportunistically supplemented with specimens sorted from the standard bottom trawl sample (30 min duration) to achieve target sample sizes. Specimens were classified by length group (≤10 cm or >10 – 20 cm) and apportioned among three types of laboratory analyses: (1) otolith age and growth (Matta and Kimura, 2012); (2) biochemistry (total lipids) (Copeman et al., 2016); (3) diet (stomach contents) (Yeung and Yang, 2017). The sample sizes by each species-year-station combination for otolith, lipids, and diet analysis are summarized in Supplementary Table S1. Specimens for otoliths and biochemistry were frozen at ≤-20°F, and those for diet were preserved in 10% formalin. All specimens were thawed (if frozen), blotted dry, weighed to 0.001 g, and length was measured to 1 mm before submitting to different specialized laboratories for their respective analyses.

2.2.2 Benthic sampling

A benthic grab (0.1-m^2 Day Grab[a], KC Denmark A/S) was used to collect duplicate sediment samples at selected stations to sample infauna (Table S1). Each infaunal sample was washed through a 1-mm mesh screen. The retained portion was fixed in 10% buffered formalin with rose Bengal stain for 2 – 3 days, then drained and preserved in 50% isopropyl alcohol. A portion (~200 – 400 mL) of a third sample was

analyzed by a Malvern Mastersizer 2000[a] laser particle sizer for surficial sediment grain size (Yeung and Yang, 2018).

Infauna were not sampled at every station where fish samples were collected in 2016 – 2018 (Table S1). To fill in these gaps, infaunal data collected in other years (2006 – 2014, 2019; (Yeung, unpublished data; Yeung and Yang, 2018; Yeung et al., 2010) at or near these 2016 – 2018 stations with missing infaunal data were used as proxies. These are the best available data in the study area from recent years. They were collected with the same type of sampler. Replicates from same or different years, where available, were averaged to reduce spatial and/or temporal variation. In the Bering Sea where infauna data are scant, such proxies can be useful at the coarse taxonomic resolution presented here for the characterization of the prey field on a broad spatial scale (Gray and Elliott, 2009). Infaunal assemblages are not generally known to vary significantly within the interannual time scale (Ysebaert and Herman, 2002). Retrospective analyses of historical data did not show that climate change has caused significant differences in eastern Bering Sea infauna biomass at the aggregate taxonomic resolution examined in this study (Coyle et al., 2007), nor in the northern Bering Sea (Norton Sound) epifauna community (Jewett et al., 2005).

2.2.3 Bottom temperature

Bottom temperature was measured with a conductivity-temperature-depth (CTD) sensor attached to the bottom trawl during fishing. The present warm stanza began around late 2013, and in 2016 the average bottom temperature in the eastern Bering Sea survey area reached a record high. The bottom temperature cooled in 2017 and environmental conditions — including winter sea ice extent, winds, air and ocean temperatures, were considered average (Stabeno et al., 2017). Warm temperatures returned in 2018 (NPFMC, 2018), again causing the cold pool to almost disappear (Lauth et al., 2019). According to this thermal history, juvenile flatfish from age-0 to age-4 collected in 2016 — 2018 experienced warm-stanza conditions throughout most if not their entire lives (Table 1).

169

170 2.3 Biological indices

171 2.3.1 Juvenile densities

172 High densities of juveniles may indicate high habitat quality (Gilliers et al., 2006). Since the shelter and
173 diet requirements of NRS and YFS are very similar, the densities of each species within a given area may
174 also reflect the intensity of competition for habitat resources. The densities (number of fish per hectare)
175 of juvenile NRS and YFS at each station where a beam trawl sample was taken were respectively
176 estimated from the concurrent bottom trawl sample as indicators of habitat quality. Although the beam
177 trawl may be more efficient in capturing juvenile flatfish, the effort was not as rigorously standardized as
178 for the bottom trawl, which at minimum estimates relative densities.

179

180 2.3.2 Prey composition

181 The prey-specific index of relative importance (*PSIRI*) (Brown et al., 2012) was calculated to characterize
182 prey availability and composition in the habitat (grab samples) and diet (stomach samples):

183 $PSIRI_i = \frac{FO_i \times (\%PN_i + \%PW_i)}{2} = \frac{\%N + \%W}{2}$,

184 where prey-specific average percent abundance $\%PA_i = \frac{\sum_{j=1}^{n} \%A_{ij}}{n_i}$, frequency of occurrence $FO_i = \frac{n_i}{n}$,
185 $\%A_{ij}$ = % abundance (by count N or weight W) of prey group i in stomach or grab sample j, n_i = the
186 number of stomach (grab) samples containing prey group i, and n = the total number of stomach (grab)
187 samples.

188

189 The prey energy index (*Prey*) converts prey composition into caloric values to characterize prey quality in
190 the habitat:

191 $Prey = \sum_{i=1}^{m} PSIRI_i \times C_i$,

where C = mean energy content (kJ·g^{-1} WWT) of prey group i. The C of polychaetes (2.9), clams (3.9), amphipods (4.9), and "other" (5.6) – a category combining cumaceans, crangonid shrimps, and echinoderms, were determined from bomb calorimetry in a previous study (Yeung and Yang, 2018).

2.3.3 Age and growth

Otoliths were removed from the fish and stored in glycerin/thymol solution (Forsberg, 2001) to hydrate them and enhance contrast between growth zones. Otoliths were aged from surface patterns using a dissecting stereomicroscope; age estimates were confirmed using the break-and-burn technique for those otoliths without clear surface patterns (Matta and Kimura, 2012). Digital photographs were taken of whole otoliths viewed under reflected light (Supplementary Figure S1). ImagePro[a] software (Media Cybernetics) was used to measure otolith length (*OL*) from the anterior to posterior tip of the left otolith. Linear models of *TL* ~ *OL* + *Area* + *OL*×*Area* were fit to the data from each species to determine if there were differences between collection areas in otolith growth relative to body growth. On the right otolith, a measurement axis was drafted from the core to the anterior margin, and annual increment (annulus) widths (*OW*) were delineated perpendicular to the anterior distal edge of each translucent growth zone. Widths of the first (*OW*-1) and second (*OW*-2) increments were graphed with respect to area and year of formation for both species using boxplots.

A growth index (*Growth*) was calculated for each otolith-aged fish as its length divided by the mean length of all fish of its age (Werner et al., 2019). Age-length keys were constructed for each species using the methods of Isermann and Knight (2005) as implemented in the R statistical software (R Core Team, 2020) *FSA* package (Ogle, 2016), in which the proportion of age-a, P(a_l), where a = 1, …, k in each 1-cm interval l = 2, …, 20 cm, was determined from the otolith analysis. The key was used to assign age to specimens in the catch that were not aged by otolith analysis. An unaged fish of $TL = l$ has the probability P(a_l) of being assigned age-a.

217

218 2.3.4 Physiological condition indices

219 2.3.4.1 Morphometric

220 The scaled mass index (*SMI*) of body condition was calculated for 2080 juveniles (2016: 741 NRS, 270 YFS;
221 2017: 248 NRS, 272 YFS; 2018: 363 NRS, 186 YFS; Table S1). The *SMI* removes the effects of ontogenetic
222 growth on the length-weight relationship through standardization to the same growth phase; that is,
223 length (Peig and Green, 2010):

224 $$SMI = W \times \left[\frac{TL_0}{TL}\right]^b,$$

225 where SMI = predicted weight when TL is standardized to TL_0, W = weight, TL = length, TL_0 =
226 standardized length, defined here as 10 cm – approximately the mean length of the juveniles analyzed,
227 and b = slope from standard major axis regression of $\log_{10} W$ on $\log_{10} TL$.

228

229 Unlike the *Growth* index, the *SMI* is not age-based and incorporates weight. The two indices offer
230 complementary perspectives on the fitness of fish: *Growth* is useful for comparing structural growth that
231 may affect susceptibility to predation and forage ability – advantages in survivorship conferred by more
232 rapidly reaching greater sizes; the *SMI* is useful for inferring overwintering success and starvation
233 resistance – advantages conferred by greater mass relative to length.

234

235 2.3.4.2 Biochemical

236 Juvenile flatfish specimens were stored at -20°C until processing, at which point the specimens were
237 thawed, blotted dry, and whole bodies were weighed (WWT, 0.1 mg) and measured for total length,
238 standard length, and body depth (*TL*, *SL*, *BD*, 0.1 mm). Fish intestinal tracts and internal organs were then
239 removed and muscle tissue was sampled from up to fifteen individuals at a range of sizes for each species
240 per station. For fish larger than 50 mm *SL*, muscle tissue was sampled by first removing the skin along the
241 dorsal margin and then dissecting ~300 mg WWT of dorsal muscle. Fish smaller than 50 mm *SL* were

sampled by removing all of the skin, head, and internal organs, and all remaining muscle tissues were used for lipid analyses to have adequate sample strength. Tissue samples were immediately placed on ice and within 1 h, were stored in chloroform under nitrogen in a -20°C freezer for later extraction and lipid class analyses. Lipids were extracted from each sample (n = 287 – 2017: 53 NRS, 92 YFS; 2018: 102 NRS, 40 YFS) in a 2:1 chloroform:methanol solution using a modified Folch procedure (Folch et al., 1957; Parrish, 1987). Lipid classes were analyzed using thin-layer chromatography with flame ionization detection (TLC-FID) and a MARK VI Iatroscan[a] (Iatron Laboratories, Tokyo, Japan) (Copeman et al., 2016). Absolute amounts of four lipid classes (triacylglycerols, free fatty acids, sterols, and polar lipids) were quantified using calibration curves on lipid class standards and summed into total lipids per WWT (μg mg^{-1}) (Copeman et al., 2016) as an index of energetic condition (Fraser, 1989).

2.4 Statistical analysis

2.4.1 Analysis of variance

Distance-based permutational analysis of variance (PERMANOVA) was used to evaluate differences in growth and condition responses between groups. Significance was determined by 999 random permutations based on the distance matrix. Significant results of interest were further analyzed with post-hoc pairwise *t*-tests between groups. The analyses were conducted using the PRIMER v7 +PERMANOVA computer package (Anderson et al., 2008; Clarke et al., 2014)

PERMANOVA was used to test year and area effects (Type III sum of squares, permutation of residuals under a reduced model) on each univariate response of length (*Growth*), otolith size (*OL*, *OW*) at age, scaled mass index (*SMI*), and total lipid content (*Lipids*; Table 2). It was also used to test year and area effects on the multivariate response of diet composition (*PSIRI*). The condition indices and diet composition, which were not associated with otolith-validated ages, were averaged by length (cm interval) within each station. Univariate responses were Euclidean-transformed; diet composition was Bray-Curtis transformed. PERMANOVA produces a distance-based pseudo-*F* statistic that is analogous to

268 the classical ANOVA *F*-statistic. In the case of one response variable using Euclidean distance, pseudo-*F* is
269 the same as the univariate ANOVA *F* statistic, but where *p*-values are obtained by permutation, thus
270 avoiding the assumption of normality (Anderson, 2017). The PERMANOVA routine can handle unbalanced
271 experimental design. However, differences in within-group dispersion for experiments with small and
272 unequal group sizes can confound the test of different group locations (centroids) (Anderson et al., 2008).
273 Therefore, significant difference between groups is considered conservatively (at $p < 0.01$) and with the
274 support of graphical data plots.
275
276 The ANOSIM $\underline{R}$ statistic (PRIMER v7) (Clarke et al., 2014) was used to test the similarity in prey
277 composition between diet and infauna. Prey composition was represented by the *PSIRI* values of the four
278 major prey groups, transformed into Bray-Curtis distance. The null hypothesis of no difference between
279 compositions was rejected if <5% of the total number of simulated $\underline{R}$ values was greater than or equal to
280 the observed $\underline{R}$ value. $\underline{R}$ values generally lie between 0 and +1, with a value of 0 representing the null
281 hypothesis, a value close to +1 indicating high dissimilarity, and a negative value close to 0 indicating
282 within group dissimilarity (Chapman and Underwood, 1999). A two-way ANOSIM model was first used to
283 test for diet differences between length classes of each species nested within area. The fish were divided
284 into two length classes *Lenclass*: 1 – ≤10 cm; 2 – >10 cm, approximately dividing at age-2 for NRS and age-
285 3 for YFS, and corresponding to warm-year versus cold-year cohorts (Table 1). If the length effect was not
286 significant, lengths were pooled for one-way ANOSIM to test for similarity between diet and infauna by
287 area (stations as replicates).
288
289 2.4.2 Condition-habitat relationship
290 Regression models were used to explore whether variability in growth or condition was related to
291 differences in habitat characteristics (Table 2). The indices *SMI*, *Growth*, and *Lipids* were modeled as
292 separate responses. There was no correlation between *SMI* and *Growth* (Pearson $r = 0.05$, $n = 507$), or
293 *SMI* and *Lipids* ($r = 0$, $n = 281$). The model was fitted to the average response within a station, with *Length*

(cm interval) as a covariate. The continuous habitat quality predictors considered were bottom temperature (*Temp*), mean sediment grain size (*Sed*), prey energy index (*Prey*, log-transformed as habitat predictor), and juvenile densities (*NRS*, *YFS*). Pairwise scatterplots of the variables included in the models were first examined for outliers and possible functional relationships to guide the analysis. Pairwise scatterplots and correlations between predictors were used to screen for collinearity. Bottom temperature was selected over depth from the onset because of the high correlation between them (r = -0.71, n = 64), and the well-known bioenergetic relationship between temperature and physiological condition (e.g, Stevens et al., 2006). The sample size n in each species-area treatment block varied by response: *Lipids* 4 – 22; *SMI* 13 – 58; *Growth* 26 – 77. The sample size for each response was highest in the south for NRS but lowest in the south for YFS. Samples were pooled across years since they were only available in the northern Bering Sea in 2017, and the thermal environment that the year variable was intended to represent – that is, whether the year was "warm" or "cold", was already directly represented by the bottom temperature variable.

The response variables *SMI*, *Growth*, and *Lipids* (Table 2) were approximately normally distributed. Preliminary analysis showed that interaction between the selected predictors for modeling was not significant, but pairwise scatterplots did not clearly assert linear relationships between response and predictor. Given the low sample size and relatively narrow range for each predictor, generalized linear models (GLM) without interactions were evaluated for each species as starting models (R Core Team, 2020). If there were non-linear patterns in the GLM diagnostics, generalized additive models (GAM) were also evaluated to compare with the GLMs. Models with Gaussian (identity link) and gamma (log link) distributed dependent variables were compared:

$y_i \sim N(\mu_i, \sigma^2)$, $\mathbf{E}(y_i) \sim \mu_i$, $\text{var}(y_i) = \sigma^2$,

$\mu_i = \text{Intercept} + Length_i + NRS_i + YFS_i + Prey_i + Temp_i + Sed_i$,

or

$y_i \sim Gamma(\mu_i, \tau)$, $\mathbf{E}(y_i) \sim \mu_i$, $\text{var}(y_i) = \mu_i^2/\tau$,

320 $\log(\mu_i) = \text{Intercept} + Length_i + NRS_i + YFS_i + Prey_i + Temp_i + Sed_i$,

321 where the response $Y = \{y_1, .., y_n\}$ was either the average *SMI*, *Growth*, or *Lipids* index of fish of length l at

322 a station.

323

324 The best of all possible combinations of predictors for each response was identified based on the Bayesian

325 Information Criterion (BIC) (Schwarz, 1978), and models were re-fitted with the further removal of any

326 predictor that was not significant at the 5% level. Diagnostics (e.g. residuals, fitted values, Cook's

327 distance) were performed on the best models with significant relationships to check for violation of model

328 assumptions (Zuur et al., 2014). Similar steps were used to select the best GLM or GAM between

329 Gaussian and gamma distributions (Zuur, 2012). The R *mgcv* package (Wood, 2017) was used to fit GAMs

330 with thin plate regression splines. Model selection between the best GLMs and GAMs using the BIC was

331 conducted using the R *MuMIn* package (Bartón, 2020).

332

333 3 RESULTS

334 3.1 Prey composition in flatfish diets and the infauna

335 A total of 755 NRS and 344 YFS non-empty stomachs were analyzed from 2016 to 2018 (Table S1). Based

336 on the *PSIRI*, polychaetes were the most important prey for NRS, whereas for YFS "other" prey were also

337 important in addition to polychaetes (Supplementary Table S2). These "other" prey consisted primarily of

338 mysid shrimps and cumaceans. For both species, amphipods were more important to smaller juveniles.

339 For the diet of NRS, neither length class *Lenclass* (pseudo-$F_{1,54} = 0.27$, $p = 0.82$), *Year* (pseudo-$F_{2,54} = 2.11$,

340 $p = 0.06$), nor *Area* (pseudo-$F_{2,54} = 2.18$, $p = 0.05$) had significant effects. For the diet of YFS, *Lenclass*

341 (pseudo-$F_{1,40} = 2.69$, $p = 0.05$) and *Area* (pseudo-$F_{2,40} = 0.68$, $p = 0.65$) effects were also not significant, and

342 *Year* effect was marginal (pseudo-$F_{2,40} = 3.04$, $p = 0.01$), driven mainly by the relatively lower proportions

343 of amphipods and clams in the diet in 2018 than other years (Table S2).

344

345 The spatial difference in infaunal assemblage (pseudo-$F_{2,147}$ = 3.08, p = 0.02) was mostly due to the
346 prevalence of polychaetes in the north relative to the south (t = 1.81, p = 0.03) (Figure 2). The central
347 area shared characteristics with both the north (t = 1.75, p = 0.05) and the south (t = 1.69, p = 0.05).
348 Polychaetes dominated the infaunal composition in each area, similar to the diet compositions (Table S2).
349 The composition of "other" prey varied by area. This category was most diverse in the south, where the
350 three most dominant taxa were echinoderms, holothuroids, and echiurids; in the central area, the three
351 most dominant taxa were foraminifera, gastropods, and echiurids; in the north, they were foraminifera,
352 tunicates, and sipunculids. The prey energy index *Prey* increased towards the north (south = 1188, central
353 = 1870, north = 2509 kJ·g^{-1}).
354
355 3.2 Diet-Prey Correspondence
356 For NRS, there was a significant difference between diet and prey infauna compositions in the south but
357 not in the central or the north (south: $\underline{R}$ = 0.23, p = 0.001; central: $\underline{R}$ = -0.07, p = 0.91; north: $\underline{R}$ = -0.15, p =
358 0.85). For YFS, there was a significant difference between diet and prey compositions in the south and
359 the north (south: $\underline{R}$ = 0.34, p = 0.002; central: $\underline{R}$ = -0.05, p = 0.88; north: $\underline{R}$ = 0.11, p = 0.02). There were no
360 significant differences in diet composition between NRS and YFS in any of the areas (south: $\underline{R}$ = 0.13, p =
361 0.05; central: $\underline{R}$ = 0.02, p = 0.27; north: $\underline{R}$ = -0.23, p = 0.92) (Figure 2). Overall, differences were weak even
362 if significant ($\underline{R} \lesssim 0.3$). The components of the "other" prey group were different between the diets and
363 the infauna, which may indicate the different sampling efficiencies of a predator versus a mechanical
364 grab. In YFS diet, for example, "other" prey consisted mainly of motile shrimps and cumaceans, whereas
365 "other" in the infauna were mainly slower-moving groups such as echinoderms.
366
367 3.3 Age and growth
368 A total of 182, 50, and 116 NRS and 63, 21, and 77 YFS were aged by otoliths, respectively, in 2016, 2017,
369 and 2018 (Table S1). There were no samples from the north. Fish collected for otolith analysis ranged in

length from 2.7 – 17.7 cm for NRS and 4.8 – 15.7 cm for YFS. Almost 100% of NRS were age-1 to age-2; the oldest fish was age-4; 90% of YFS were age-2 to age-3; the oldest fish was age-9.

The effects of *Year* (NRS: pseudo-$F_{2,342}$ = 47, p = 0.001; YFS: pseudo-$F_{2,155}$ = 8, p = 0.004) and *Area* (NRS: pseudo-$F_{1,342}$ = 91, p = 0.001; YFS: pseudo-$F_{1,155}$ = 10, p = 0.004) on *Growth* were significant for both species. The *Year–Area* interaction was significant for NRS but not for YFS (NRS: pseudo-$F_{2,342}$ = 28, p = 0.001; YFS: pseudo-$F_{2,155}$ = 3, p = 0.08). *Growth* was significantly higher in the south than the central area but showed a decline from 2016 to 2018, to being almost the same in both areas by 2018 (Figure 3). Since the *Area* effect was important, separate age-length keys were developed for each species in the south and central area. The age-length key from the central area was applied to the north since no northern fish were aged.

Otolith length was highly correlated with body length for each species-area group (r = 0.95 – 0.97). The correlation between the otolith length of a fish of age-*a* and each of its component annual otolith increment widths was generally low (r = -0.15 – 0.36). Otolith length may track body length more closely because both integrate growth conditions over the lifetime, whereas *OW* tracks conditions in a specific growth year, such that the correlation with body length may be more variable.

For NRS, the first and second otolith increment widths were significantly associated with the *Year of formation* (*OW*-1, 2012 – 2017: pseudo-$F_{5,331}$ = 17, p = 0.001; *OW*-2, 2013 – 2017: pseudo-$F_{4,156}$ = 16, p = 0.001) and *Area* (*OW*-1: pseudo-$F_{1,331}$ = 43, p = 0.001; *OW*-2: pseudo-$F_{1,156}$ = 32, p = 0.001). For YFS, the *Year of formation* effect was also significant (*OW*-1, pseudo-$F_{5,146}$ = 4, p = 0.003; *OW*-2, pseudo-$F_{4,138}$ = 10, p = 0.001). The *Area* effect was only significant on the second increment (*OW*-1, pseudo-$F_{1,146}$ = 0, p = 0.74; *OW*-2, pseudo-$F_{1,138}$ = 11, p = 0.001).

The first increment width (*OW*-1) of NRS peaked around 2015 – 2016 in both the south and central areas, then decreased sharply in 2017; *OW*-2 decreased from 2015 onward. The *OW*-1 of YFS increased from 2014 to 2017 in both areas, but *OW*-2 showed an opposite, decreasing trend in the same period (Figure 4). Simple linear regression of increment width on the mean bottom temperature (Table 1) in the year of its formation by species and area (not shown) indicated slightly positive trends for YFS in the south (regression slope coefficient $b = 0.08$, $p = 0.002$, $r = 0.30$) and the central ($b = 0.08$, $p < 0.001$, $r = 0.32$), and for NRS in the south ($b = 0.06$, $p < 0.001$, $r = 0.33$). However, there was no significant trend for NRS in the central area ($b = 0.01$, $p = 0.34$, $r = 0$).

3.4 Somatic growth and body condition

The scaled mass index (*SMI*) of each species was not correlated with length ($r \approx -0.1$, $p > 0.1$). The effects of *Year* (NRS: pseudo-$F_{2,1346} = 38$, $p = 0.001$; YFS: pseudo-$F_{2,721} = 58$, $p = 0.001$), *Area* (NRS: pseudo-$F_{2,1346} = 19$, $p = 0.001$; YFS: pseudo-$F_{2,721} = 4$, $p = 0.01$) and *Year-Area* interaction (NRS: pseudo- $F_{2,1346} = 16$, $p = 0.001$; YFS: pseudo- $F_{2,721} = 9$, $p = 0.001$) were significant on the *SMI* of both species. The mean *SMI* of both species generally increased towards the north. It also increased from 2016 to 2017, then decreased slightly from 2017 to 2018 (Figure 5).

The *Lipids* index had a higher correlation with the length of YFS than with NRS (NRS, $r = -0.18$, $p = 0.03$, n = 149; YFS, $r = -0.46$, $p < 0.01$, n = 132). The residuals of *Lipids* regressed on length of NRS were not associated with *Year* (pseudo-$F_{1,195} = 0$) or *Area* (pseudo-$F_{2,194} = 0.2$, $p = 0.7$). The effects of *Year* (pseudo-$F_{1,176} = 8$, $p = 0.02$) and *Area* (pseudo-$F_{2,176} = 6$, $p = 0.02$) on the *Lipids* residuals of YFS were also weak. For both species, *Lipids* increased from 2017 to 2018 in the central area, but decreased from 2017 to 2018 in the south, overall reversing the pattern of *Lipids* from being higher in the south to higher in the central within the two years (Figure 6).

3.5 Variation in growth and body condition between habitats

The selected best models were generally valid according to diagnostics, except for the scaled mass index (*SMI*) and the *Lipids* index of NRS. The best models for these two responses seriously violated assumptions, and explained only 5% (*SMI* = *Length* + *Temp*) and 8% (*Lipids* = *Length*) of the deviance (Table 3). They are nonetheless reported for completeness. The best model for the *Lipids* index of YFS included all six predictors and had 86% of the deviance explained, which may suggest model overfitting given the relatively low sample size (*n* = 65).

Length was a significant predictor in every best model of growth and condition response (Table 3, Figure 7). For both species, *Length* was positively related to *Growth* and negatively related to the *SMI* and *Lipids* indices. Both species had the same predictors for *Growth* (*Growth* = *Length* + *NRS* + *Sed*) and the general relationships between *Growth* with each of the predictors were similar. Temperature (*Temp*) was significant in the *SMI* and *Lipids* models of YFS. The relationship was linear and negative with *SMI*, but nonlinear with *Lipids.* However, both response indices had a negative relationship with *Temp* in the range of 6 to 9^{o}C, where data were densest. For models that included mean sediment grain size (*Sed*) as a significant predictor, the response tended to peak over the medium grain size range. Juvenile densities of either *NRS* or *YFS* were significant in all the valid models, whereas the prey energy index (*Prey*) only appeared in one.

4 DISCUSSION

We found evidence of spatial and temporal variation in the somatic growth and condition of juvenile flatfishes in the Bering Sea during the period of 2016 to 2018. Juveniles of both species grew faster in length and to larger length-at age in the south than in the central area of the Bering Sea. The positive relationship between otolith increment width and summer bottom temperature suggests that larger size is associated with warmer temperature, since otolith and somatic lengths are highly correlated.

Here, the relationship between increment width and temperature seems to be stronger for juvenile YFS than NRS. The increment widths of adult NRS and YFS in the eastern Bering Sea were also positively correlated with summer bottom temperatures, and the relationship was similarly stronger for YFS (r = 0.90) than for NRS (r = 0.59) (Matta et al., 2010). Otolith increment widths can reflect variability within a fish's environment at annual and subannual time scales (Campana and Neilson, 1985), and numerous studies in recent years have employed otolith increment chronologies to demonstrate strong effects of temperature on growth of many marine species (e.g., Morrongiello et al., 2012). A follow-up otolith chronology study focused solely on adult YFS found subtle differences in otolith and somatic growth across a latitudinal gradient within the Bering Sea, suggesting heterogeneity in climate impacts growth of these flatfishes across the region (Matta et al., 2016).

Yellowfin sole are abundant in the northern Bering Sea. The center of the YFS population is in the central area, and its abundance in the south is relatively low (Hamazaki et al., 2005; NOAA, 1987). The stock structure of YFS in the Bering Sea is currently unknown, and it is unclear whether YFS in the northern and eastern Bering Seas constitute separate populations (Spies et al., 2019). Conversely, there have not been reports of any substantial presence of NRS north of 60^{o} until recently (Lauth et al., 2019), possibly because surveys that target NRS in that area only began in 2010 (Stevenson and Lauth, 2019). The distributions of juvenile NRS and YFS overlap mainly in the central area (Yeung and Cooper, 2019).

Inferring from their more northerly distribution, YFS may be adapted to colder habitats and more sensitive to increasing temperatures than NRS. Juvenile specimens are only available from the northern Bering Sea in 2017, and NRS are relatively rare there. Based on these limited data, the morphometric-based condition of juvenile YFS appears to be better in the northern Bering Sea, while the condition of juvenile NRS also improves towards the north. The exploratory habitat models in this study show that the biochemical and morphometric condition of juvenile YFS may be negatively influenced by temperature.

While warmer temperatures may be associated with faster growth in juvenile flatfish in this study, there is suggestion that the trend may not continue if the current high temperatures persist or further warming occurs in their habitat. Mean growth was significantly higher in the south than the central area in 2016 and 2017, but in 2018 there was no difference between the areas, due primarily to decreased growth in the south. A counter-argument would be that the decreased growth in the south in 2018 reflected the negative effects of the colder temperatures of 2017 on the cumulative growth of the juveniles (mostly age-1 to age-2 of NRS and age-2 to age-3 of YFS). However, otolith increment widths also suggest a decrease in growth around 2016, the warmest year in the life history of these juveniles. In the Barents Sea, the record-warm conditions in 2016 were associated with higher abundance and larger age-0 individuals of fishes including the flatfish *Hippoglossoides platessoides* (Eriksen et al., 2020). Age-0 fish are rare in our study. If the Barents Sea effects of 2016 apply to the Bering Sea, they may manifest in the 2017 age-1 and 2018 age-2 groups, but that is not supported by otolith growth. Instead, the decreased somatic and otolith growth in juvenile flatfishes over the period of this study suggest that the Bering Sea may be approaching the upper thermal limit for optimum growth at the shallow nursery habitats. As we gather more otolith data we may be able to infer from the increments if there is a point where the growth and temperature relationship becomes nonlinear (that is, otolith growth decreases after reaching the thermal maximum).

The maximum bottom temperature observed during our study and input into our models was 13.4^{o}C. The average summer bottom temperatures in 2019 were higher than in 2018 by 1.7^{o}C in the south, 0.8^{o}C in the central, and 2.7^{o}C in the northern Bering Sea, according to AFSC bottom trawl survey data. The magnitude of warming was even greater in the coastal northern Bering Sea. Norton Sound, important for northern Bering Sea fisheries and potentially a YFS nursery (Yeung, unpublished data), experienced a maximum bottom temperature above 15^{o}C in the summer of 2019 (Zacher et al., 2020). It is unknown whether optimal growth in the field can still be realized by juvenile flatfish, especially the cold-adapted YFS, at such high temperatures. There have been laboratory and field studies on the physiological effects

498 of temperature on juvenile NRS (age-0) (Hurst et al., 2010), but there is no comparable literature on
499 juvenile YFS. Laboratory studies have found increased growth potential in age-0 NRS at temperatures
500 between 2 and 13^{o}C when food was not limiting (Hurst and Abookire, 2006; Hurst et al., 2010). Adult
501 flatfishes along the U.S. North Pacific coast typically have higher condition during cooler climate stanzas
502 (Keller et al., 2013). Arctic cod abundance increased in the southern Chukchi Sea in 2017, but their energy
503 content has decreased (Huntington et al., 2020). Juvenile YFS production may initially be favored by
504 warmer temperatures in the northern Bering Sea, but if warming continues, growth and condition may
505 deteriorate and negatively affect future recruitment and production. The short time-series in this study
506 with the interposition of a cold year between two warm ones was likely to have confounding effects on
507 biological responses. If the warming persists, spatial patterns in the distribution and energetics may
508 become clearer.
509
510 We measured a decrease in muscle lipid content with fish length, which may signify that juvenile fish were
511 in a rapid growth phase. Elevated nursery temperatures and high predation pressure have been
512 hypothesized to account for a decrease in lipid density with length in age-0 juvenile Atlantic cod (*Gadus*
513 *morhua*) during their settlement into nearshore cold-water nursery habitat (Copeman et al., 2008). In
514 juveniles, energy is allocated between growth and lipid storage. Growth can reduce size-dependent
515 mortality and predation pressure (Sogard, 1997; Suthers, 1998). Lipid storage can also promote near-
516 term survivability of the individual and future reproductive and recruitment success of the population
517 (Adams, 1999). Under high food availability, lipid content generally increases with body size during the
518 juvenile phase (Martin et al., 2017). In principle, lower activity and higher lipid content are selected for at
519 colder temperatures (Pörtner, 2002). Previous studies on larval Arctic cod and walleye pollock larvae
520 showed that the thermal optima for lipid-based condition factors were lower than those for
521 morphometric-based condition factors (Koenker et al., 2018). Another study focused on juvenile English
522 sole (*Parophrys vetulus*) condition metrics in an estuary found that similarly sized age-0 fish were in higher
523 energetic condition at cold downriver sites, but in higher morphometric-based condition at warmer

524 upriver sites (Stowell et al., 2019). The authors hypothesized that this may have been due in part to the
525 direct physiological effects of warmer temperatures at upriver sites, but they could not rule out
526 differences in prey quality along the marine to freshwater gradient. Further research is needed to
527 understand the direct (temperature) and indirect (prey quality, predation pressure) effects of warming
528 oceanographic conditions on lipid-based and morphometric-based condition in juvenile flatfish. The
529 relationships between the different types of condition indices and selection of the most appropriate and
530 informative condition index for juvenile flatfishes in the Bering Sea are also important topics for further
531 research (Gilliers et al., 2006; McPherson et al., 2010; Schloesser and Fabrizio, 2017).
532
533 Prey energy was not an important factor in juvenile growth and condition in this study; juvenile flatfish
534 densities, which can reflect predation pressure, were significant factors. There was no evidence that prey
535 resources were limiting across the Bering Sea, although the spatial mismatch between the infauna prey
536 and the diet compositions (Manly et al., 2002) of juvenile NRS and YFS in the central area suggests lower
537 prey availability there than in the other two areas. Yeung and Yang (2017, 2018) similarly concluded that
538 the south may have higher prey resources than the central area based on this premise. The central area
539 may have lower prey resources because in this area NRS and YFS distributions have the greatest overlap
540 and therefore higher predation pressure. Conversely, the northern Bering Sea may have higher prey
541 resources because it is mostly inhabited only by YFS. How prey and consumer indices are related to
542 growth and condition of juvenile flatfish is speculative until there is a better understanding of predator-
543 prey interactions within these habitats.
544
545 Whether juvenile NRS and YFS will become more abundant in the northern Bering Sea given suitable
546 habitat depends on complicated early life history dynamics such as spawning location, larval duration and
547 oceanic current transport (Cooper et al., 2014; Duffy-Anderson et al., 2015), and other potentially
548 significant habitat variables such as dissolved oxygen and salinity (Sobocinski et al., 2018; Yamashita et al.,
549 2001) that may be altered under a changing ecosystem. Although in recent years the inshore areas of the

550 northern Bering Sea have been warmer than comparable areas in the south in the summer (Lauth et al.,
551 2019; Zacher et al., 2020), fish growth and energetic condition may still lag because of lower light
552 intensity, colder winter temperatures, or other unknown seasonal environmental differences.
553
554 This study provides a baseline for the growth and condition (morphometric- and lipid-based) of juvenile
555 flatfish in the Bering Sea. The acquisition of these data using the large-scale, systematic Bering Sea
556 bottom trawl surveys is a relatively recent development. Although NRS have moved northward of their
557 historical range in the eastern Bering Sea, they are still not abundant in the northern Bering Sea (Yeung
558 and Cooper, 2019). For this reason, there is a lack of data in the northern Bering Sea for a more
559 comprehensive long-term comparison. Additional condition data from the northern Bering Sea are
560 required to better test the quality of this habitat for juvenile flatfish and its contribution to biomass
561 production. The serious implications of the rapid changes in the subarctic and arctic oceans for human
562 societies (Huntington et al., 2020) provide an incentive to regularly conduct Bering Sea surveys, and for
563 the long-term monitoring that is key to understanding climate change effects on marine population
564 dynamics (Brown et al., 2019; Capotondi et al., 2019; van der Veer et al., 2015).
565
566 [a]Reference to trade names does not imply endorsement by the National Marine Fisheries Service, NOAA.
567
568 5 ACKNOWLEDGMENTS
569 This work was supported by grants for Essential Fish Habitat research from the NMFS Alaska Regional
570 Office. We thank Carlissa Salant and Michelle Stowell in the Marine Lipid Ecology Laboratory at the
571 Hatfield Marine Science Center for conducting the lipid analyses; Captain Steve Elliot of the F/V
572 *Vesteraalen* and his crew of Robert Butlay, Sean Harrigan, Andy Wenger, and others, and the scientists
573 who participated in the Alaska Fisheries Science Center bottom trawl surveys for their dedication and
574 expertise.
575

576 6 LITERATURE CITED

577 Abookire, A.A., Rose, C.S., 2005. Modifications to a plumb staff beam trawl for sampling uneven, complex
578 habitats. Fish. Res. 71, 247-254.

579 Adams, S.M., 1999. Ecological role of lipids in the health and success of fish populations, in: Arts, M.T.,
580 Wainman, B.C. (Eds.), Lipids in freshwater ecosystems. Springer New York, New York, NY, pp. 132-160.

581 Amara, R., Meziane, T., Gilliers, C., Hermel, G., Laffargue, P., 2007. Growth and condition indices in
582 juvenile sole *Solea solea* measured to assess the quality of essential fish habitat. Mar. Ecol. Prog. Ser. 351,
583 201-208.

584 Anderson, M., Gorley, R.N., Clarke, K., 2008. PERMANOVA+ for primer: Guide to software and statistical
585 methods.

586 Anderson, M.J., 2017. Permutational Multivariate Analysis of Variance (PERMANOVA), in: Balakrishnan,
587 N., Colton, T., Everitt, B., Piegorsch, W., Ruggeri, F., Teugels, J.L. (Eds.), Wiley StatsRef: Statistics Reference
588 Online, pp. 1-15.

589 Bartón, K., 2020. MuMIn: Multi-Model Inference. R package version 1.43.17. https://CRAN.R-
590 project.org/package=MuMIn.

591 Brown, C.J., Broadley, A., Adame, M.F., Branch, T.A., Turschwell, M.P., Connolly, R.M., 2019. The
592 assessment of fishery status depends on fish habitats. Fish and Fisheries 20, 1-14.

593 Brown, S.C., Bizzarro, J.J., Cailliet, G.M., Ebert, D.A., 2012. Breaking with tradition: redefining measures for
594 diet description with a case study of the Aleutian skate *Bathyraja aleutica* (Gilbert 1896). Environ. Biol.
595 Fish. 95, 3-20.

596 Brown, Z.W., Arrigo, K.R., 2013. Sea ice impacts on spring bloom dynamics and net primary production in
597 the eastern Bering Sea. J. Geophys. Res.-Oceans 118, 43-62.

598 Campana, S.E., Neilson, J.D., 1985. Microstructure of fish otoliths. Can. J. Fish. Aquat. Sci. 42, 1014-1032.

599 Capotondi, A., Jacox, M., Bowler, C., Kavanaugh, M., Lehodey, P., Barrie, D., Brodie, S., Chaffron, S., Cheng,
600 W., Dias, D.F., Eveillard, D., Guidi, L., Iudicone, D., Lovenduski, N.S., Nye, J.A., Ortiz, I., Pirhalla, D., Pozo
601 Buil, M., Saba, V., Sheridan, S., Siedlecki, S., Subramanian, A., de Vargas, C., Di Lorenzo, E., Doney, S.C.,
602 Hermann, A.J., Joyce, T., Merrifield, M., Miller, A.J., Not, F., Pesant, S., 2019. Observational needs
603 supporting marine ecosystems modeling and forecasting: from the global ocean to regional and coastal
604 systems. Front. Mar. Sci. 6.

605 Chapman, M.G., Underwood, A.J., 1999. Ecological patterns in multivariate assemblages: information and
606 interpretation of negative values in ANOSIM tests. Mar. Ecol. Prog. Ser. 180, 257-265.

607 Clarke, K.R., Gorley, R.N., Somerfield, P.J., Warwick, R.M., 2014. Change in marine communities: an
608 approach to statistical analysis and interpretation, 3rd ed. PRIMER-E Ltd, Plymouth, UK.

609 Cooper, D.W., Duffy-Anderson, J.T., Norcross, B.L., Holladay, B.A., Stabeno, P., 2014. Northern rock sole
610 (*Lepidopsetta polyxystra*) juvenile nursery areas in the eastern Bering Sea in relation to hydrography and
611 thermal regimes. ICES J. Mar. Sci. 71, 1683-1695.

612 Cooper, D.W., Nichol, D.G., 2016. Juvenile northern rock sole (*Lepidopsetta polyxystra*) spatial distribution
613 and abundance patterns in the eastern Bering Sea: spatially-dependent production linked to temperature.
614 ICES J. Mar. Sci. 73, 1138-1146.

615 Copeman, L.A., Laurel, B.J., Boswell, K.M., Sremba, A.L., Klinck, K., Heintz, R.A., Vollenweider, J.J., Helser,
616 T.E., Spencer, M.L., 2016. Ontogenetic and spatial variability in trophic biomarkers of juvenile saffron cod
617 (*Eleginus gracilis*) from the Beaufort, Chukchi and Bering Seas. Polar Biol. 39, 1109-1126.

618 Copeman, L.A., Parrish, C.C., Gregory, R.S., Wells, J.S., 2008. Decreased lipid storage in juvenile Atlantic
619 cod (*Gadus morhua*) during settlement in cold-water eelgrass habitat. Mar. Biol. 154, 823-832.

620 Coyle, K.O., Konar, B., Blanchard, A., Highsmith, R.C., Carroll, J., Carroll, M., Denisenko, S.G., Sirenko, B.I.,
621 2007. Potential effects of temperature on the benthic infaunal community on the southeastern Bering Sea
622 shelf: possible impacts of climate change. Deep Sea Research Part II: Topical Studies in Oceanography 54,
623 2885-2905.

624 De Raedemaecker, F., Brophy, D., O'Connor, I., Comerford, S., 2012. Habitat characteristics promoting
625 high density and condition of juvenile flatfish at nursery grounds on the west coast of Ireland. J. Sea Res.
626 73, 7-17.

627 Duffy-Anderson, J.T., Bailey, K.M., Cabral, H.N., Nakata, H., Van der Veer, H.W., 2015. The planktonic
628 stages of flatfishes: physical and biological interactions in transport processes, in: Gibson, R.N., Nash,
629 R.D.M., Geffen, A.J., Van der Veer, H.W. (Eds.), Flatfishes: biology and exploitation, 2nd ed. John Wilery &
630 Sons, Ltd., West Sussex, UK, pp. 132-170.

631 Duffy-Anderson, J.T., Stabeno, P., III, A.G.A., Cieciel, K., Deary, A., Farley, E., Fugate, C., Harpold, C., Heintz,
632 R., Kimmel, D., Kuletz, K., Lamb, J., Paquin, M., Porter, S., Rogers, L., Spear, A., Yasumiish, E., 2019.
633 Responses of the northern Bering Sea and southeastern Bering Sea pelagic ecosystems following record-
634 breaking low winter sea ice. Geophys. Res. Lett. 46, 9833-9842.

635 Eisner, L.B., Zuenko, Y.I., Basyuk, E.O., Britt, L.L., Duffy-Anderson, J.T., Kotwicki, S., Ladd, C., Cheng, W.,
636 2020. Environmental impacts on walleye pollock (*Gadus chalcogrammus*) distribution across the Bering
637 Sea shelf. Deep-Sea Res. Pt II, 104881.

638 Eriksen, E., Bagøien, E., Strand, E., Primicerio, R., Prokhorova, T., Trofimov, A., Prokopchuk, I., 2020. The record-
639 warm Barents Sea and 0-group fish response to abnormal conditions. Front. Mar. Sci. 7, 338.

640 Feder, H.M., Jewett, S.C., Blanchard, A.L., 2007. Southeastern Chukchi Sea (Alaska) macrobenthos. Polar
641 Biol. 30, 261-275.

642 Folch, J., Lees, M., Stanley, G.H.S., 1957. A simple method for the isolation and purification of total lipids
643 from animal tissues. J. Biol. Chem. 226, 497-509.

644 Forsberg, J.E., 2001. Aging manual for Pacific halibut: Procedures and methods used at the International
645 Pacific Halibut Commission. Technical Report No. 46. International Pacific Halibut Commission, Seattle,
646 WA.

647 Fraser, A.J., 1989. Triacylglycerol content as a condition index for fish, bivalve, and crustacean larvae. Can.
648 J. Fish. Aquat. Sci. 46, 1868-1873.

649 Gibson, R., 1994. Impact of habitat quality and quantity on the recruitment of juvenile flatfishes. J. Sea
650 Res. 32, 191-206.

651 Gilliers, C., Le Pape, O., Désaunay, Y., Morin, J., Guérault, D., Amara, R., 2006. Are growth and density
652 quantitative indicators of essential fish habitat quality? An application to the common sole *Solea solea*
653 nursery grounds. Estuar. Coast. Shelf Sci. 69, 96-106.

654 Gray, J.S., Elliott, M., 2009. Ecology of marine sediments : from science to management. Oxford University
655 Press, Oxford.

656 Grebmeier, J.M., 2012. Shifting patterns of life in the Pacific Arctic and sub-Arctic Seas. Annu. Rev. Mar.
657 Sci. 4, 63-78.

658 Halas, G., Neufeld, G., 2018. An overview of the subsistence fisheries of the Bristol Bay Management Area,
659 Alaska. Alaska Department of Fish and Game Division of Subsistence, Special Publication No. BOF 2018-04.
660 http://www.adfg.alaska.gov/download/Special%20Publications/SP2_SP2018-004.pdf.

661 Hamazaki, T., Fair, L., Watson, L., Brennan, E., 2005. Analyses of Bering Sea bottom-trawl surveys in
662 Norton Sound: absence of regime shift effect on epifauna and demersal fish. ICES J. Mar. Sci. 62, 1597-
663 1602.

664 Hollowed, A.B., Planque, B., Loeng, H., 2013. Potential movement of fish and shellfish stocks from the sub-
665 Arctic to the Arctic Ocean. Fish. Oceanogr. 22, 355-370.

666 Huntington, H.P., Danielson, S.L., Wiese, F.K., Baker, M., Boveng, P., Citta, J.J., De Robertis, A., Dickson,
667 D.M.S., Farley, E., George, J.C., Iken, K., Kimmel, D.G., Kuletz, K., Ladd, C., Levine, R., Quakenbush, L.,
668 Stabeno, P., Stafford, K.M., Stockwell, D., Wilson, C., 2020. Evidence suggests potential transformation of
669 the Pacific Arctic ecosystem is underway. Nat. Clim. Change 10, 342-348.

670 Hurst, T.P., Abookire, A.A., Knoth, B., 2010. Quantifying thermal effects on contemporary growth
671 variability to predict responses to climate change in northern rock sole (*Lepidopsetta polyxystra*). Can. J.
672 Fish. Aquat. Sci. 67, 97-107.

673 Isermann, D.A., Knight, C.T., 2005. A computer program for agelength keys incorporating age assignment
674 to individual fish. N. Am. J. Fish. Manag. 25, 1153-1160.

675 Jewett, S., Hamazaki, T., Weingartner, T., Danielson, S., 2005. Retrospective analyses of Norton Sound
676 benthic fauna. University of Alaska Fairbanks,School of Fisheries and Ocean Science
677 Alaska Department of Fish and Game.

678 Keller, A.A., Bradburn, M.J., Simon, V.H., 2013. Shifts in condition and distribution of eastern North Pacific
679 flatfish along the U.S. west coast (2003-2010). Deep-Sea Res. Pt I 77, 23-35.

680 Koenker, B.L., Copeman, L.A., Laurel, B.J., 2018. Impacts of temperature and food availability on the
681 condition of larval Arctic cod (*Boreogadus saida*) and walleye pollock (*Gadus chalcogrammus*). ICES J. Mar.
682 Sci. 75, 2370-2385.

683 Kotwicki, S., Lauth, R.R., Williams, K., Goodman, S.E., 2017. Selectivity ratio: A useful tool for comparing
684 size selectivity of multiple survey gears. Fish. Res. 191, 76-86.

685 Lauth, R.R., Dawson, E.J., Conner, J., 2019. Results of the 2017 eastern and northern Bering Sea
686 continental shelf bottom trawl survey of groundfish and invertebrate fauna, U.S. Dep. Commer. NOAA
687 Tech. Memo. NMFS-AFSC-396. https://repository.library.noaa.gov/view/noaa/20734.

688 Manly, B.F.J., McDonald, L.L., Thomas, D.L., McDonald, T.L., Erickson, W.P., 2002. Resource selection by
689 animals: statistical design and analysis for field studies, 2nd ed. Kluwer Academic Publishers, Boston.

690 Martin, B., Heintz, R., Danner, E., Nisbet, R., 2017. Integrating lipid storage into general representations of fish
691 energetics. J. Anim. Ecol. 86, 812-825.

692 Matta, M., Kimura, D., 2012. Age determination manual of the Alaska Fisheries Science Center Age and
693 Growth Program. NOAA Professional Paper NMFS; 13.
694 https://repository.library.noaa.gov/view/noaa/4149.

695 Matta, M.E., Black, B.A., Wilderbuer, T.K., 2010. Climate-driven synchrony in otolith growth-increment
696 chronologies for three Bering Sea flatfish species. Mar. Ecol. Prog. Ser. 413, 137-145.

697 Matta, M.E., Helser, T.E., Black, B.A., 2016. Otolith biochronologies reveal latitudinal differences in growth
698 of Bering Sea yellowfin sole *Limanda aspera*. Polar Biol. 39, 2427-2439.

699 McDevitt, C., Koster, D., Runfola, D., Horne-Brine, M., Esquible-Hussion, J., 2020. Subsistence fisheries
700 harvest monitoring report, Kuskokwim Management Area, Alaska, 2018. Alaska Dept. of Fish and Game,
701 Division of Subsistence, Technical Paper No. 467, Alaska Dept. of Fish and Game, Division of Subsistence,
702 Nome, Alaska. http://www.adfg.alaska.gov/techpap/TP%20467.pdf.

703 McPherson, L.R., Slotte, A., Kvamme, C., Meier, S., Marshall, C.T., 2010. Inconsistencies in measurement
704 of fish condition: a comparison of four indices of fat reserves for Atlantic herring (*Clupea harengus*). ICES
705 J. Mar. Sci. 68, 52-60.

706 Morrongiello, J.R., Thresher, R.E., Smith, D.C., 2012. Aquatic biochronologies and climate change. Nat.
707 Clim. Change 2, 849-857.

708 Mueter, F., Dawe, E., Pálsson, O.I.K., 2012. Subarctic fish and crustacean populations—climate effects and
709 trophic dynamics. Mar. Ecol. Prog. Ser. 469, 191-193.

710 National Marine Fisheries Service, 2020. Fisheries of the U.S. 2018. U.S. Department of Commerce, NOAA
711 Current Fishery Statistics No. 2018. Silver Spring, Maryland.
712 https://www.fisheries.noaa.gov/national/commercial-fishing/fisheries-united-states-2018.

713 Nichol, D.G., Kotwicki, S., Wilderbuer, T.K., Lauth, R.R., Ianelli, J.N., 2019. Availability of yellowfin sole
714 *Limanda aspera* to the eastern Bering Sea trawl survey and its effect on estimates of survey biomass. Fish.
715 Res. 211, 319-330.

716 NOAA, 1987. Bering, Chukchi, and Beaufort seas: coastal and ocean zones strategic assessment. U.S. Dep.
717 Commer. NOAA, National Ocean Service, Ocean Assessments Division, Strategic Assessment Branch,
718 Rockville, Maryland.

719 NOAA, 2014. NOAA's Arctic Action Plan – supporting the national strategy for the Arctic region. U.S. Dep.
720 Commer., NOAA, Silver Spring, Maryland. https://arctic.noaa.gov/Arctic-
721 News/ArtMID/5556/ArticleID/308/NOAAs-Arctic-Action-Plan.

722 NPFMC, 2017. Essential Fish Habitat (EFH) 5-year review summary report.
723 https://alaskafisheries.noaa.gov/sites/default/files/2015efh_5yearreview.pdf.

724 NPFMC, 2018. Ecosystem status report 2018. Eastern Bering Sea. December 2018.
725 https://access.afsc.noaa.gov/reem/ecoweb/pdf/2018ecosysEBS-508.pdf.

Ogle, D.H., 2016. Introductory fisheries analyses with R, 1st ed. CRC Press, Boca Raton, Florida.

Parrish, C.C., 1987. Separation of aquatic lipid classes by chromarod thin-layer chromatography with measurement by Iatroscan flame ionization detection. Can. J. Fish. Aquat. Sci. 44, 722-731.

Peig, J., Green, A.J., 2010. The paradigm of body condition: a critical reappraisal of current methods based on mass and length. Funct. Ecol. 24, 1323-1332.

Pörtner, H.O., 2002. Physiological basis of temperature-dependent biogeography: trade-offs in muscle design and performance in polar ectotherms. J. Exp. Biol. 205, 2217-2230.

R Core Team, 2020. R: A language and environment for statistical computing. R Foundation for Statistical Computing, Vienna, Austria.

Renner, M., Huntington, H.P., 2014. Connecting subsistence harvest and marine ecology: A cluster analysis of communities by fishing and hunting patterns. Deep-Sea Res. Pt II 109, 293-299.

Schloesser, R.W., Fabrizio, M.C., 2017. Condition indices as surrogates of energy density and lipid content in juveniles of three fish species. Trans. Am. Fish. Soc. 146, 1058-1069.

Schwarz, G., 1978. Estimating the dimension of a model. Ann. Statist. 6, 461-464.

Sobocinski, K.L., Ciannelli, L., Wakefield, W.W., Yergey, M.E., Johnson-Colegrove, A., 2018. Distribution and abundance of juvenile demersal fishes in relation to summer hypoxia and other environmental variables in coastal Oregon, USA. Estuar. Coast. Shelf Sci. 205, 75-90.

Sogard, S.M., 1997. Size-selective mortality in the juvenile stage of teleost fishes: a review. . Bull. Mar. Sci. 60, 1129– 1157.

Spies, I., Wilderbuer, T., Nichol, D.G., Ianelli, J., 2019. Assessment of the yellowfin sole stock in the Bering Sea and Aleutian Islands. 2019 North Pacific groundfish stock assessment and fishery evaluation reports for 2020. https://archive.afsc.noaa.gov/refm/stocks/plan_team/2019/BSAIyfin.pdf.

Stabeno, P.J., Bell, S.W., 2019. Extreme conditions in the Bering Sea (2017–2018): Record-breaking low sea-ice extent. Geophys. Res. Lett. 46, 8952-8959.

Stabeno, P.J., Duffy-Anderson, J.T., Eisner, L.B., Farley, E.V., Heintz, R.A., Mordy, C.W., 2017. Return of warm conditions in the southeastern Bering Sea: Physics to fluorescence. PLOS ONE 12, e0185464.

Stabeno, P.J., Farley, E.V., Jr., Kachel, N.B., Moore, S., Mordy, C.W., Napp, J.M., Overland, J.E., Pinchuk, A.I., Sigler, M.F., 2012. A comparison of the physics of the northern and southern shelves of the eastern Bering Sea and some implications for the ecosystem. Deep-Sea Res. Pt II 65-70, 14-30.

Stabeno, P.J., Thoman, R.L., Wood, K., 2019. Recent warming in the Bering Sea and its impact on the ecosystem. December 6, 2019. https://arctic.noaa.gov/Report-Card/Report-Card-2019/ArtMID/7916/ArticleID/846. .

Stevens, M., Maes, J., Ollevier, F., 2006. A bioenergetics model for juvenile flounder *Platichthys flesus*. J. Appl. Ichthyol. 22, 79-84.

Stevenson, D.E., Lauth, R.R., 2019. Bottom trawl surveys in the northern Bering Sea indicate recent shifts in the distribution of marine species. Polar Biol. 42, 407-421.

762 Stoner, A.W., Titgen, R.H., 2003. Biological structures and bottom type influence habitat choices made by
763 Alaska flatfishes. J. Exp. Mar. Biol. Ecol. 292, 43-59.

764 Stowell, M.A., Copeman, L.A., Ciannelli, L., 2019. Variability in juvenile English sole condition relative to
765 temperature and trophic dynamics along an Oregon estuarine gradient. Estuar. Coast 42, 1955-1968.

766 Suthers, I.M., 1998. Bigger? Fatter? Or is faster growth better? Considerations on condition in larval and
767 juvenile coral-reef fish. Aust. J. Ecol. 23, 265-273.

768 van der Veer, H.W., Dapper, R., Henderson, P.A., Jung, A.S., Philippart, C.J.M., Witte, J.I.J., Zuur, A.F., 2015.
769 Changes over 50 years in fish fauna of a temperate coastal sea: Degradation of trophic structure and
770 nursery function. Estuar. Coast. Shelf Sci. 155, 156-166.

771 Werner, K.M., Taylor, M.H., Diekmann, R., Lloret, J., Möllmann, C., Primicerio, R., Fock, H.O., 2019.
772 Evidence for limited adaptive responsiveness to large-scale spatial variation of habitat quality. Mar. Ecol.
773 Prog. Ser. 629, 179-191.

774 Wood, S.N., 2017. Generalized Additive Models: An Introduction with R, 2nd ed. Chapman & Hall/CRC
775 Texts in Statistical Science, Boca Raton.

776 Wyllie-Echeverria, T., Wooster, W.S., 1998. Year-to-year variations in Bering Sea ice cover and some
777 consequences for fish distributions. Fish. Oceanogr. 7, 159-170.

778 Yamashita, Y., Tanaka, M., Miller, J.M., 2001. Ecophysiology of juvenile flatfish in nursery grounds. J. Sea
779 Res. 45, 205-218.

780 Yeung, C., Cooper, D.W., 2019. Contrasting the variability in spatial distribution of two juvenile flatfishes in
781 relation to thermal stanzas in the eastern Bering Sea. ICES J. Mar. Sci. 77, 953-963.

782 Yeung, C., Yang, M.-S., 2017. Habitat quality of the coastal southeastern Bering Sea for juvenile flatfishes
783 from the relationships between diet, body condition and prey availability. J. Sea Res. 119, 17-27.

784 Yeung, C., Yang, M.-S., 2018. Spatial variation in habitat quality for juvenile flatfish in the southeastern
785 Bering Sea and its implications for productivity in a warming ecosystem. J. Sea Res. 139, 62-72.

786 Yeung, C., Yang, M.-S., McConnaughey, R.A., 2010. Polychaete community in south-eastern Bering Sea in
787 relation to groundfish distribution and diet. J. Mar. Biol. Assoc. UK 90, 903-917.

788 Ysebaert, T., Herman, P.M.J., 2002. Spatial and temporal variation in benthic macrofauna and
789 relationships with environmental variables in an estuarine, intertidal soft-sediment environment. Mar.
790 Ecol. Prog. Ser. 244, 105-124.

791 Zacher, L.S., Richar, J.I., Foy, R.J., 2020. The 2019 eastern and northern Bering Sea continental shelf
792 bottom trawl survey: Results for commercial crab species., U.S. Dep. Commer. NOAA Tech. Memo. NMFS-
793 AFSC-399. https://repository.library.noaa.gov/view/noaa/22919.

794 Zuur, A., 2012. A beginner's guide to Generalized Additive Models with R. Highland Statistics Ltd,
795 Newburgh, UK.

796 Zuur, A., Hilbe, J., Ieno, E., 2014. Beginner's guide to GLM and GLMM with R. Highland Statistics Ltd,
797 Newburgh, UK.
798

799

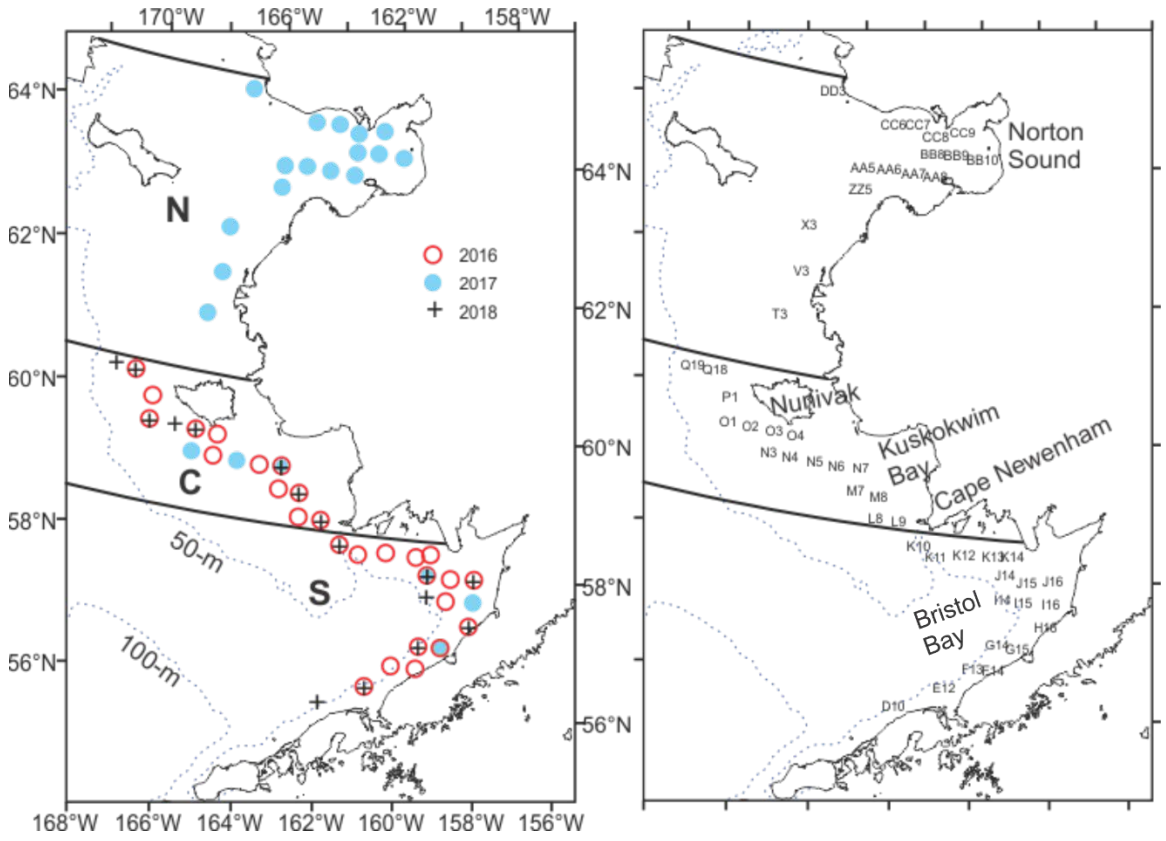

Figure 1. Stations sampled for juvenile northern rock sole and yellowfin sole in 2016, 2017, and 2018 on the inner shelf of the Bering Sea, which is divided latitudinally (bold lines) into the south (S), central (C), and north (N) areas for this study (left panel). Station names are referenced (right panel). The types and numbers of samples collected at each station are summarized in Supplementary Table S1.

809

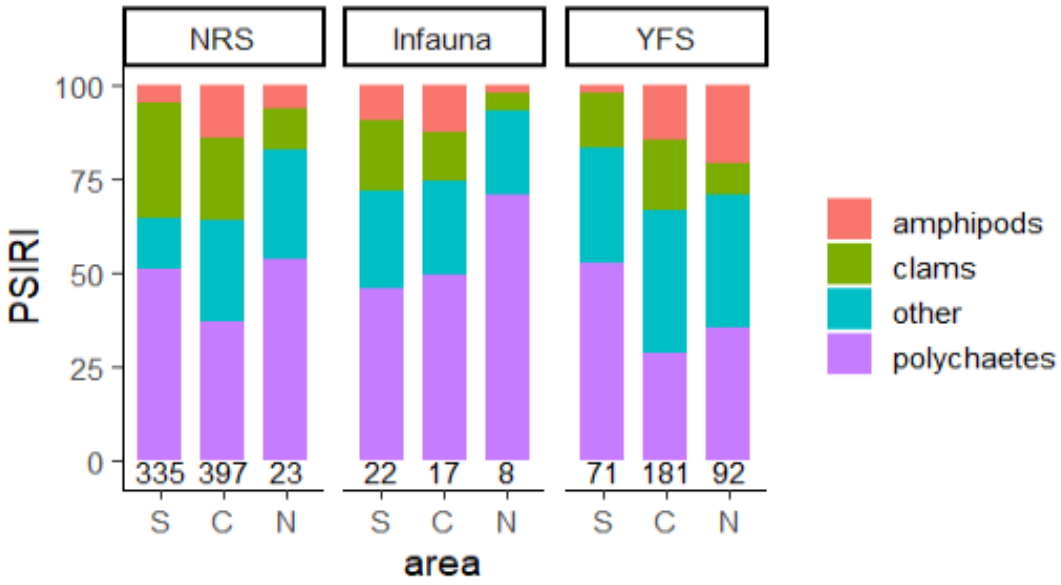

810

811 Figure 2. Prey-specific index of relative importance (*PSIRI*) of prey groups in the diets of northern rock

812 sole (NRS) and yellowfin sole (YFS), and in the infaunal assemblage, by area: south (S), central (C), and

813 north (N). The sample size (number of NRS, YFS stomachs; number of infauna sample stations) for each

814 area is given below the bar.

815

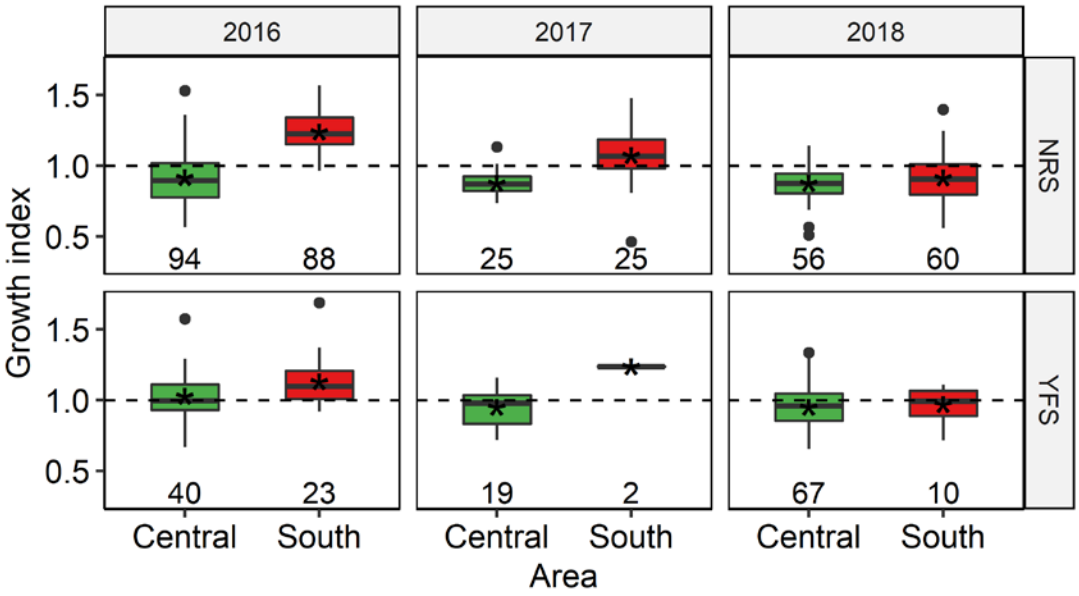

Figure 3. Box-whisker plots of the *Growth* index of northern rock sole (NRS) and yellowfin sole (YFS) by area and year. There are no samples from the north area for this analysis. Box limits are the 25% and 75% quantiles; bold line is the median; asterisk is the mean; whiskers show values within 1.5 times the interquartile range; dots are outliers. The sample size is given below the box.

Figure 4. Box-whisker plots of otolith increment width at year of formation for northern rock sole (NRS) and yellowfin sole (YFS) ranging from age-1 to age-4 by area. There are no samples from the north area for this analysis. Box limits are the 25% and 75% quantiles; bold line is the median; asterisk is the mean; whiskers show values within 1.5 times the interquartile range; dots are outliers. The sample size is given below the box.

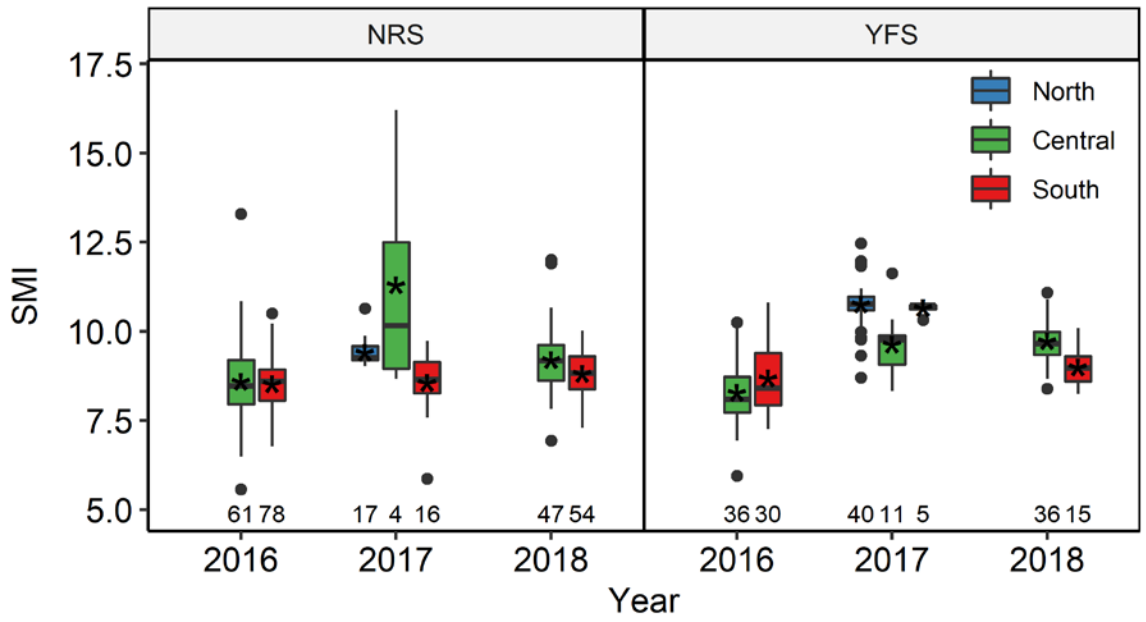

831

832 Figure 5. Box-whisker plots of the scaled mass index (*SMI*) for northern rock sole (NRS) and yellowfin sole
833 (YFS) by area and year. Box limits are the 25% and 75% quantiles; bold line is the median; asterisk is the
834 mean; whiskers show values within 1.5 times the interquartile range; dots are outliers. The sample size is
835 given below the box.

836

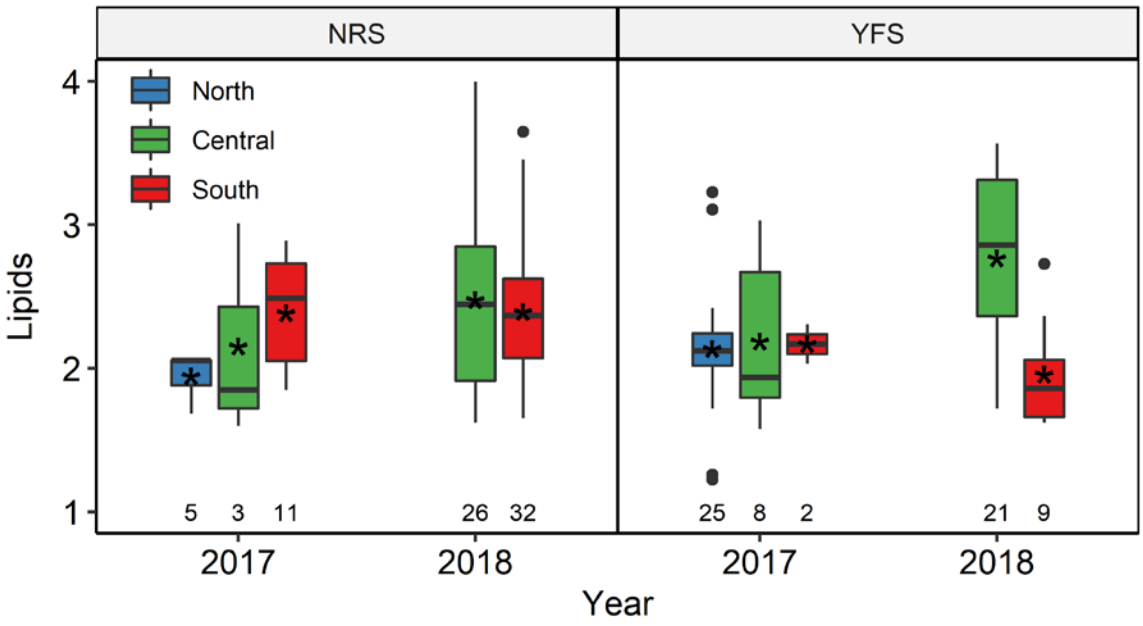

837

838 Figure 6. Box-whisker plots of the *Lipids* index for northern rock sole (NRS) and yellowfin sole (YFS) by
839 area and year. There are no 2016 samples for this analysis. Box limits are the 25% and 75% quantiles;
840 bold line is the median; asterisk is the mean; whiskers show values within 1.5 times the interquartile
841 range, dots are outliers. The sample size is given below the box. This same figure is replicated with the
842 total lipids concentration per wet weight (µg mg^{-1}; before log-transformation to the *Lipids* index) as the y-
843 variable in Supplementary Figure S2.

844

(a) Northern rock sole: *SMI* = *Length* + *Temp*

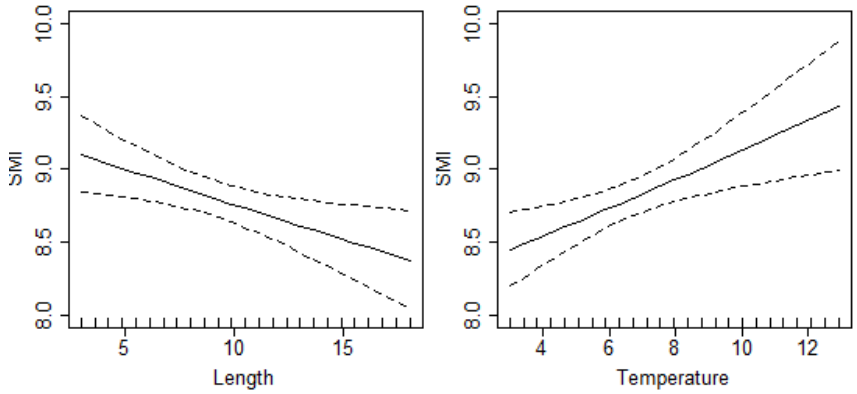

(b) Northern rock sole: *Lipids* = *Length*

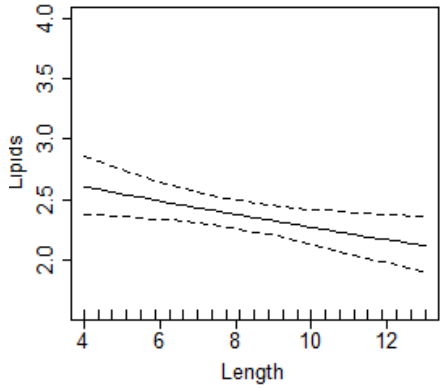

(c) Northern rock sole: *Growth* = *Length* + *NRS* + *Sed*

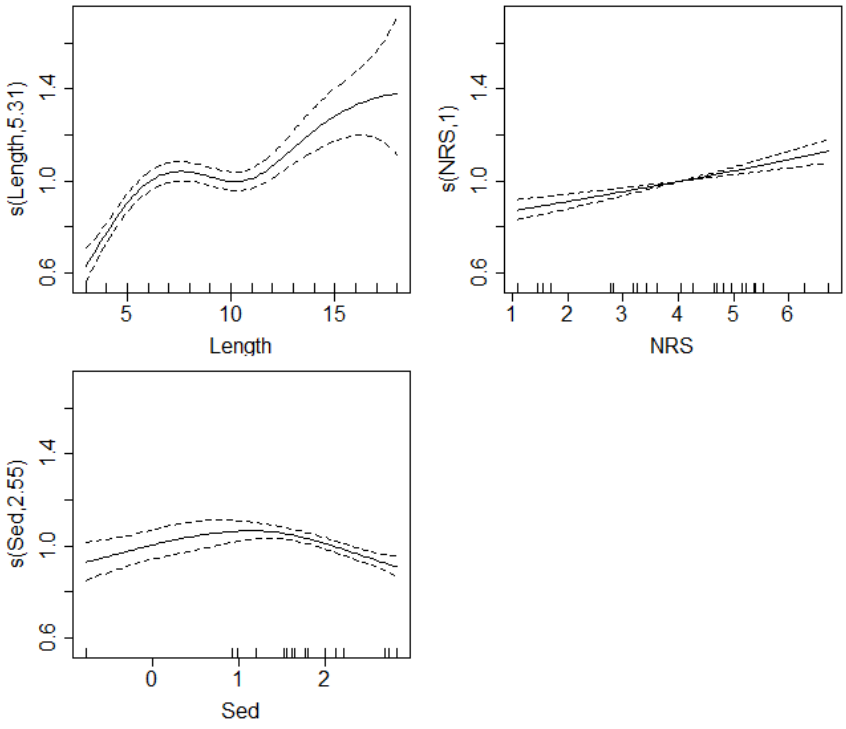

(d) Yellowfin sole: *SMI = Temp + Sed + YFS + Length*

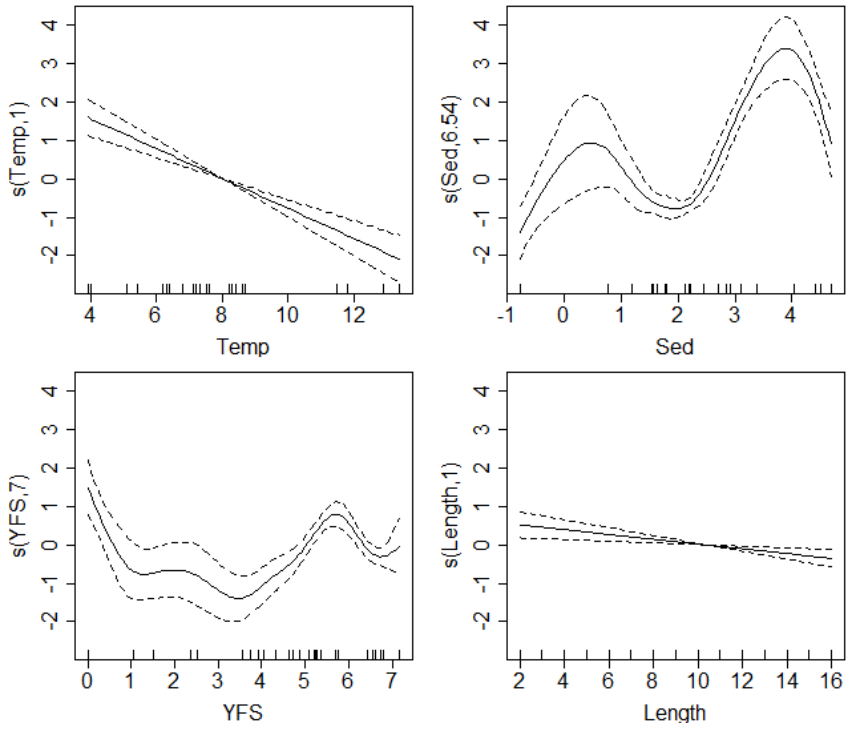

867 (e) Yellowfin sole: *Lipids* = *Length* + *Temp* + *NRS* + *Prey* + *YFS* + *Sed*

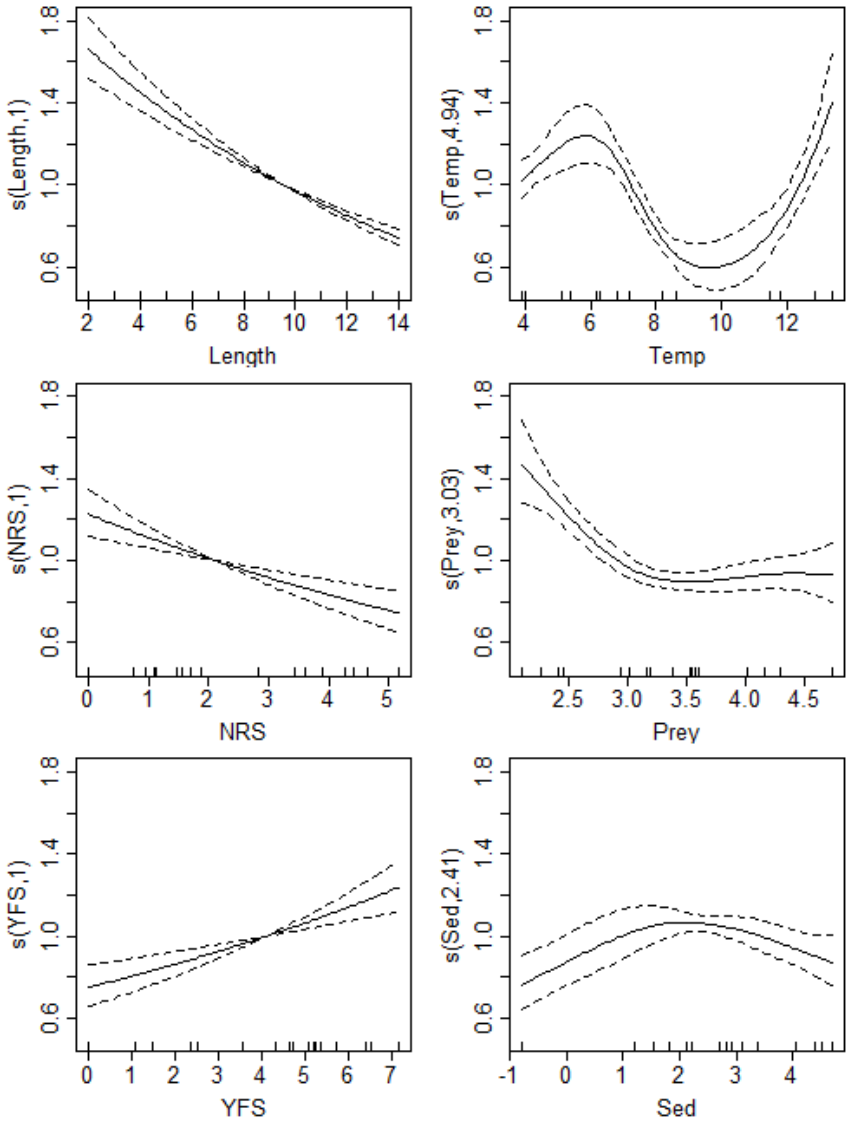

868

869

870

871

872

873

874

(f) Yellowfin sole*: Growth = Length + NRS + Sed*

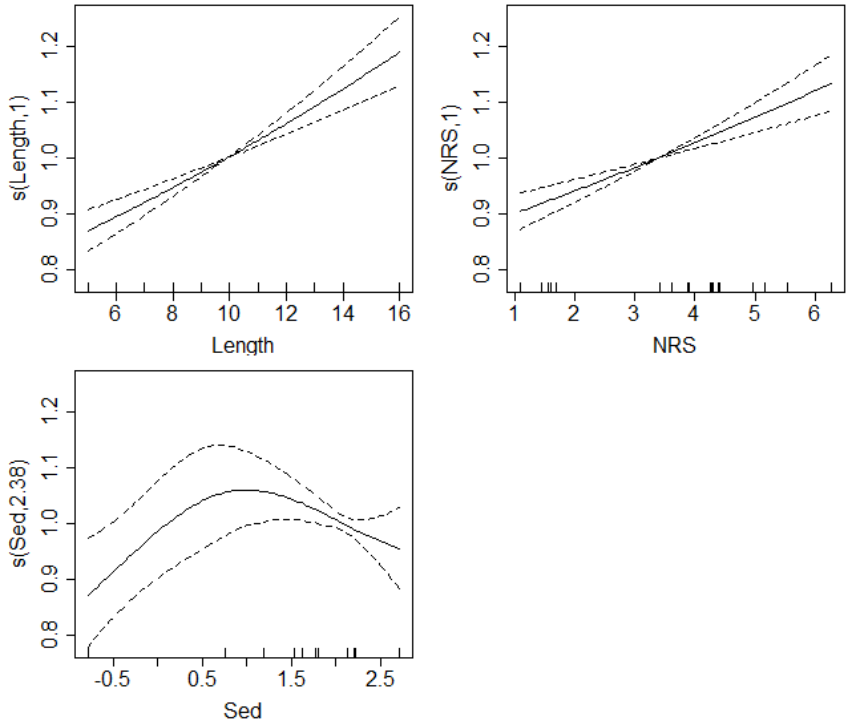

Figure 7. Best model (GLM or GAM) for the scaled mass index (*SMI*), *Lipids* and *Growth* indices of northern rock sole (NRS) and yellowfin sole (YFS). The estimated predictor function (solid) is shown on the response scale versus each predictor in the model with the 95% confidence intervals (dashed), while other continuous predictors in the model, if they exist, are set to their average values. Inward tick marks on the x-axis indicate where observations of the x variable are available. Summary of the models are given in Table 3. Explanation of the predictors is given in Table 2.

885 Table 1. (a) Birth year of flatfish of age-*a* collected each year from 2016 to 2018, coded to indicate the
886 corresponding thermal life history (red/bold – warm; blue/italic – cold; black/regular – average); for
887 example, fish of age-2 collected in 2016 had 2014, a warm year, as birth year, and had lived entirely
888 within a warm stanza 2014 – 2016, whereas an age-4 fish collected in 2016 had 2012, a cold year as birth
889 year, and had spent its first two years, 2012 – 2013, in a cold stanza, and after that in a warm stanza 2014
890 – 2016. (b) Mean summer (June – August) bottom temperature (°C) in each Bering Sea area from 2010 to
891 2018, and the area mean for that time period.
892

(a)

Age	0	1	2	3	4	5
Collection year						
2018	**2018**	2017	**2016**	**2015**	**2014**	*2013*
2017	2017	**2016**	**2015**	**2014**	*2013*	*2012*
2016	**2016**	**2015**	**2014**	*2013*	*2012*	*2011*

893

(b)

Year	2010	2011	2012	2013	2014	2015	2016	2017	2018	mean
Area										
North	2.9							6.1	4.8	4.6
Central	1.7	3.6	1.6	3.5	3.8	4.5	5.7	4.8	5.7	3.9
South	3.0	3.8	3.2	3.5	5.5	5.1	7.2	4.7	5.3	4.6

894
895

Table 2. Variables in full condition-habitat regression model.

Variable	Description	Range (untransformed)	Unit
Response			
SMI	Scaled mass index	5.355 – 18.414	–
Growth	Growth index	0.510 – 1.687	–
Lipids	log(Total lipids concentration per wet weight)	1.331 – 54.424	$\mu g\ mg^{-1}$
Predictor			
Abiotic:			
Temp	Bottom temperature	3.0 – 13.4	^{o}C
Sed	Mean grain size of surficial sediment	-0.785 – 4.697	ϕ
Biotic:			
Length	Total length	2 – 18	cm
Prey	Prey energy index	3 – 407	$kJ \cdot g^{-1}$
NRS	log(Density + 1) NRS juveniles in bottom trawl	0 – 821	no. ha^{-1}
YFS	log(Density + 1) YFS juveniles in bottom trawl	0 – 1407	no. ha^{-1}

900 Table 3. Summary of the best (GLM or GAM) models for the relationships between condition indices
901 (scaled mass index (*SMI)*, *Lipids*, *Growth*) of northern rock sole (a-c) and yellowfin sole (d-f) and habitat
902 variables. The log link function was used in gamma models, and the identity link function in Gaussian
903 models (edf – effective degrees of freedom; *n* – sample size). See section 2.4.2 for detailed methods.

(a) Northern rock sole
SMI = Length + Temp
GLM Gamma

	Estimate	Std. Error	*t*	*p*
Intercept	2.15	0.03	73.1	0.00
Length	-0.01	0.00	-2.66	0.01
Temp	0.01	0.00	3.06	0.00
Deviance explained = 5%				*n* = 276

(b) Northern rock sole
Lipids = Length
GLM Gamma

	Estimate	Std. Error	*t*	*p*
Intercept	1.05	0.08	13.1	0.00
Length	-0.02	0.01	-2.42	0.02
Deviance explained = 8%				*n* = 76

(c) Northern rock sole
Growth = Length + NRS + Sed
GAM Gamma

	Estimate	Std. Error	*t*	*p*
Intercept	-0.03	0.01	-2.57	0.01
Approximate significance of smooth terms:				
	edf	*F*	*p*	
Length	5.31	18.3	0.00	
NRS	1	28.9	0.00	
Sed	2.55	7.61	0.00	
Deviance explained = 65%				*n* = 147

(d) Yellowfin sole
SMI = Temp + Sed + YFS + Length
GAM Gaussian

	Estimate	Std. Error	*t*	*p*
Intercept	9.44	0.06	169	0.00
Approximate significance of smooth terms:				
	edf	*F*	*p*	
Temp	1	45.8	0.00	
Sed	6.54	18.6	0.00	
YFS	7	9.15	0.00	
Length	1	9.44	0.00	
Deviance explained = 66%				*n* = 173

(e) Yellowfin sole
Lipids = Length + Temp + NRS + Prey + YFS + Sed
GAM Gamma

	Estimate	Std. Error	*t*	*p*
Intercept	0.82	0.01	65	0.00
Approximate significance of smooth terms:				
	edf	*F*	*p*	
Length	1	132	0.00	
Temp	4.94	20.2	0.00	
NRS	1	19.5	0.00	
Prey	3.03	15.3	0.00	
YFS	1	18	0.00	
Sed	2.41	11.1	0.00	
Deviance explained = 86%				*n* = 65

(f) Yellowfin sole
Growth = Length + NRS + Sed
GAM Gamma

	Estimate	Std. Error	*t*	*p*
Intercept	0.02	0.01	1.57	0.12
Approximate significance of smooth terms:				
	edf	*F*	*p*	
Length	1	43.9	0.00	
NRS	1	31.5	0.00	
Sed	2.38	3.68	0.01	
Deviance explained = 61%				*n* = 70

904

905

906 SUPPLEMENTARY MATERIAL
907

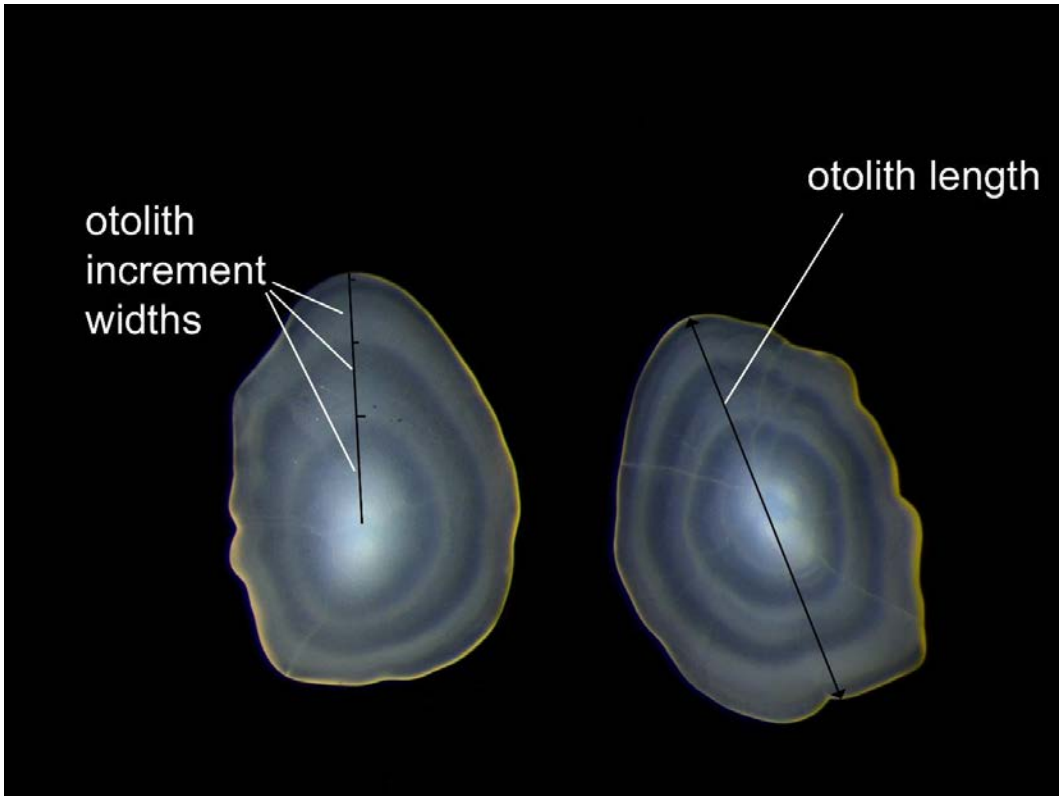

908

909

910 Figure S1. Digital image of sagittal otoliths from a 3-year-old northern rock sole showing length and

911 increment width measurements.

912

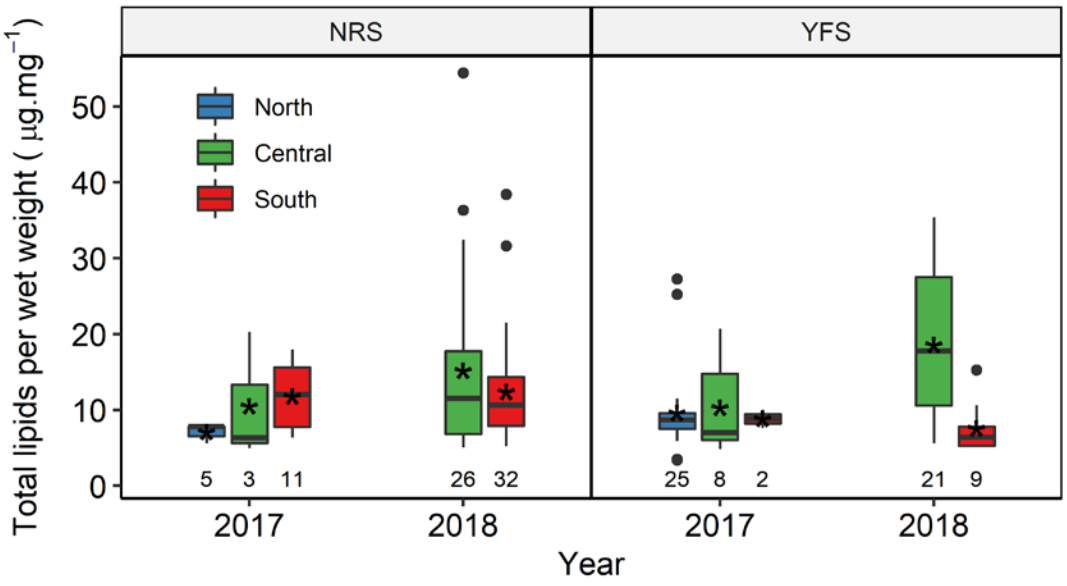

913

914 Figure S2. Box-whisker plots of the total lipids concentration per wet weight for northern rock sole (NRS)

915 and yellowfin sole (YFS) by area and year. There are no 2016 samples for this analysis. Box limits are the

916 25% and 75% quantiles; bold line is the median; asterisk is the mean; whiskers show values within 1.5

917 times the interquartile range, dots are outliers. The sample size is given below the box.

Table S1. Sample sizes of otolith, lipids, diet, and length-weight measurements for the scaled mass index (*SMI*) of juvenile flatfish (NRS = northern rock sole, YFS = yellowfin sole) by year and station in the south (S), central (C) and north (N) Bering Sea areas from 2016 to 2018, and whether infaunal data was available at the station from the same year (x), or from another year between 2006 and 2019 (+). Sediment type is abbreviated by the first letter: Gravel, Sand, Mud; the second sediment type is dominant in double-lettered codes.

							NRS				YFS			
Year	Station	Area	Depth (m)	Temp (°C)	Sediment type	Infauna	Age	Lipids	Diet	*SMI*	Age	Lipids	Diet	*SMI*
2016	F13	S	59	5.7	S	+	19		25	44				
2016	F14	S	36	6.6	S	x	12		25	37				
2016	G14	S	56	5.8	S	+	24		50	74				
2016	G15	S	30	7.5	GS	x	11		16	26				
2016	H16	S	30	7.3	SG	+			41	41			8	8
2016	J14	S	42	6.8	S	+			14	14	3		15	18
2016	J15	S	42	7.1	S	+			29	29				
2016	J16	S	34	7.6	S	x	15		15	30	5		26	31
2016	K10	S	46	6.9	S	+	7		31	38				
2016	K11	S	41	6.4	S	x					2			2
2016	K12	S	32	7.5	S	+					5		3	8
2016	K13	S	41	6.9							1			1
2016	K14	S	23	8.4	SG	+					7		22	29
2016	L8	C	32	7.6							6			6
2016	L9	C	27	7.6	S	+	16		34	50	7		30	37
2016	M7	C	28	8.2	S	x			41	41	5		31	36
2016	M8	C	22	8.7	S	+	15		23	38	7		9	16
2016	N4	C	24	8.3	S	x			39	39			9	9
2016	N6	C	23	9.2							15		22	
2016	O1	C	35	4.5	S	+	22		47	69				
2016	O3	C	29	7.1	S	x							32	32
2016	O4	C	22	8.4			19		42	61				
2016	P1	C	26	5.6	S	x	11		68	79				
2016	Q18	C	37	3	S	x	11		20	31				
2017	G15	S	32	5.2	GS	+	13	6	16	41				
2017	I16	S	28	4.9			12	5	15	42		1		1
2017	J14	S	37	4	S	+		10	15	30	2	2	3	7
2017	N3	C	23	4.8			15	10	16	48	2			2
2017	N5	C	15	6.4	S	+	6	10	14	40	6	6	6	18
2017	N7	C	16	8.2	S	+	4	4		8	11	10		25
2017	T3	N	15	11.8	S	x		5	6	12		11	15	32
2017	V3	N	16	11.8	MS	+		3	7	9		5	10	22
2017	X3	N	21	8.6	SM	x						6	12	29
2017	ZZ5	N	11	11.5	SM	x						4	2	6
2017	AA5	N	18	10.8								3	3	5
2017	AA7	N	14	12.7								2	2	6

2017	AA8	N	10	13.4	MS	x						5	6	4
2017	BB10	N	14	7.1		x						4	4	11
2017	BB8	N	20	11.8								1	2	3
2017	BB9	N	18	8.1								5		9
2017	CC6	N	10	12.9	S	x	x		18	18		5	29	35
2017	CC7	N	19	11.1								12	6	30
2017	CC8	N	20	8.4								5	8	16
2017	DD3	N	20	3.9	MS	x						5	6	11
2018	D10	S	64	4.9	S	x								
2018	E12	S	48	5.8	S	x		4	2	4				
2018	G14	S	53	5.1	S	x	7	8	10	25		1		1
2018	H16	S	25	6.2	SG	+	15	8	14	37	4	4	4	12
2018	H21	S	55	5.8			4	4	5	13				
2018	I14	S	44	5.1	S	+	8	8	7	21				
2018	J14	S	38	5.1	S	x	15	8	13	35	3	3	1	7
2018	J16	S	30	6.2	S	x	11	8	10	29	3	1	1	5
2018	K10	S	41	5.4	S	+		3	2	5				
2018	L9	C	21	6.3	S	x	14	8	19	40	4	3		7
2018	M8	C	18	7.2	S	+	10	8	10	28	30	8	34	72
2018	N7	C	16	7.2	S	x	4	5	6	15	21	8	20	49
2018	O1	C	30	6.2	S	+	8	8	19	35		1		1
2018	O2	C	31	6.8	S	+					4	2	3	9
2018	O3	C	23	5.4	S	x	10	8	12	30	8	9	6	23
2018	Q18	C	36	5.7	S	+	7	6	7	20				
2018	Q19	C	43	4.4			3	8	16	26				

924

925

Table S2. The mean *PSIRI* (Prey-Specific Index of Relative Importance) of the four major prey groups in the diets of (a) northern rock sole, (b) yellowfin sole, and in (c) the infaunal assemblage by *Year*, *Area* (south (S), central (C), and north (N), and length class *Lenclass*.

(a) Northern rock sole	Year			Area			Lenclass	
	2016	2017	2018	S	C	N	1	2
Amphipod	14	7	10	9	15	6	15	8
Clam	25	16	34	31	24	9	25	29
Polychaete	39	51	46	48	37	52	42	46
Other	21	26	10	12	24	33	19	17

(b) Yellowfin sole	Year			Area			Lenclass	
	2016	2017	2018	S	C	N	1	2
Amphipod	18	18	3	17	11	19	21	10
Clam	33	9	5	20	22	9	19	15
Polychaete	28	36	47	37	33	37	35	36
Other	21	37	45	26	35	35	25	39

(c) Infauna	Area		
	S	C	N
Amphipod	11	12	15
Clam	18	15	18
Polychaete	43	41	51
Other	28	32	16